



Quantum-like influence diagrams for decision-making

Catarina Moreira ^{a,*}, Prayag Tiwari ^c, Hari Mohan Pandey ^d, Peter Bruza ^a,
Andreas Wichert ^b



^a School of Information Systems, Science and Engineering Faculty, Queensland University of Technology, Australia

^b Department of Computer Science and Engineering, Instituto Superior Técnico/INESC-ID, University of Lisbon, Portugal

^c Department of Information Engineering, University of Padova, Italy

^d Department of Computer Science, Edge Hill University, Ormskirk, United Kingdom

ARTICLE INFO

Article history:

Received 22 December 2019

Received in revised form 2 July 2020

Accepted 6 July 2020

Available online 16 July 2020

Keywords:

Quantum-like Bayesian networks

Quantum-like influence diagrams

Decision-making

Cognition

Assembly theory

ABSTRACT

This article proposes a novel and comprehensive framework on how to describe the probabilistic nature of decision-making process. We suggest extending the quantum-like Bayesian network formalism to incorporate the notion of maximum expected utility to model human paradoxical, sub-optimal and irrational decisions. What distinguishes this work is that we take advantage of the quantum interference effects produced in quantum-like Bayesian Networks during the inference process to influence the probabilities used to compute the maximum expected utility of some decision.

The proposed quantum-like decision model is able to (1) predict the probability distributions found in different experiments reported in the literature by modelling uncertainty through quantum interference, (2) to identify decisions that the decision-makers perceive to be optimal within their belief space, but that are actually irrational with respect to expected utility theory, (3) gain an understanding of how the decision-maker's beliefs evolve within a decision-making scenario. The proposed model has the potential to provide new insights in decision science, as well as having direct implications for decision support systems that deal with human data, such as in the fields of economics, finance, psychology, etc.

© 2020 Elsevier Ltd. All rights reserved.

1. Introduction

It is widely known in the literature of cognitive science and economics that when it comes to decision-making under uncertainty, humans usually choose preferences that do not maximise the expected utility theory or that are inconsistent with the axioms of expected utility theory, leading to decisions that are either sub-optimal, paradoxical or even irrational (Aerts, Gerente, Moreira, & Sozzo, 2017; Kahneman & Tversky, 1979; Tversky & Kahneman, 1983). These paradoxical decisions can result in cognitive biases (Tversky, 1977; Tversky & Kahneman, 1974), violations of major economic principles (such as the Sure Thing Principle) (Allais, 1953; Ellsberg, 1961; Savage, 1954) or violations to the laws of probability theory and logic (Busemeyer, Wang, & Townsend, 2006; Pothos & Busemeyer, 2009). In short, decades of research has found a whole range of human judgements that deviates substantially from what would be considered normatively correct according to logic or probability theory. This fact raises a significant inconsistency: current decision support

systems cannot easily accommodate sub-optimal or irrational human decisions, because they are usually built using generative learning algorithms, which are based on probability theory. Even in decision support systems based in neural networks, the goal is always to minimise a cost function and seek optimality (Lisboa & Taktak, 2006; Mazurowska et al., 2008; Simen, Cohen, & Holmes, 2006). Hence, the normative framework for "right" decision-making in such decision support systems is the axioms of probability theory. When dealing with preferences under uncertainty, it seems that models based on normative theories of rational choice tend to tell how individuals *must* choose, instead of showing how individuals *actually* choose (Machima, 2009).

Models that could take into account, not only optimal rational decisions, but also sub-optimal, irrational and paradoxical human decisions could greatly benefit decision support systems, since there would be a better alignment between the system and the decision-maker. This alignment has the potential to provide more effective decision support systems by combining the advantages of rational and so called "irrational" decisions.

A simple solution to this problem would be to use rule-based expert systems and incorporate these cognitive biases and paradoxical decisions as rules. However, that would require an *apriori* understanding and identification of the cognitive biases involved, and would also lead to a set of rules growing largely with the

* Corresponding author.

E-mail addresses: catarina.pintomoreira@qut.edu.au (C. Moreira), prayag.tiwari@dei.unipd.it (P. Tiwari), pandeyh@edgehill.ac.uk (H.M. Pandey), p.bruza@qut.edu.au (P. Bruza), andreas.wichert@tecnico.ulisboa.pt (A. Wichert).

size of the data, which is impractical. An alternative recommendation would be to rethink about the fundamental core concepts that underline generative decision models. If under uncertainty, humans make decisions that violate the laws of probability theory, then perhaps these laws are too limited to fully express human decision-making under uncertainty. A more general and flexible probability theory could provide better insights and accommodate several paradoxical findings reported in the literature without the need to know *a priori*, which cognitive biases the decision-maker is experiencing. One such general framework that has been extensively studied in the domain of human cognition is quantum probability theory (Busemeyer & Bruza, 2012). The Quantum-like Bayesian network (Moreira, Fell, Dehdashti, Bruza, & Wichert, 2020; Moreira & Wichert, 2014, 2016a) is an example of a model that is well established in the literature for predicting and accommodating paradoxical human decisions across different decision scenarios ranging from psychological experiments (Moreira & Wichert, 2016b, 2017, 2018) to real-world credit application scenarios (Moreira, Haven, Sozzo, & Wichert, 2018). The difference between the traditional Bayesian network (BN) and a quantum-like Bayesian Network (QLBN) is the way one specifies the values of the conditional probability tables. While in the traditional BNs, one uses real numbers to express probabilities, in quantum mechanics these probabilities are expressed as probability amplitudes, which are represented by complex numbers. These quantum amplitudes define the wave function, which describes the wave characteristics of a particle. The value of the wave function of a particle at a given point of space and time is related to the likelihood of the particle's being there at the time (Skinner & Binney, 2014). To make probabilistic inferences in QLBNs, one needs to convert these quantum amplitudes into real probability values through a process of measurement, which mathematically speaking, corresponds to the squared magnitude of these amplitudes (this is known as Born's rule (Busemeyer & Bruza, 2012)). In probabilistic inferences under uncertainty, where certain random variables are not observed, this measurement process will produce non-linear quantum interference terms that can attenuate the classical probabilities. Consequently, probabilistic laws such as the law of total probability may not hold, which has been used in the literature to provide a coherent explanation for paradoxes of human decision making (Busemeyer et al., 2006; Crosson, 1999; Hristova & Grinberg, 2008; Li & Taplin, 2002; Tversky & Shafir, 1992). It is important to note that traditional Bayesian networks can also accommodate all these paradoxical findings concerned with human data, however at the cost of adding latent variables, which are not clear about what they represent in terms of the decision-maker's belief space and also lead to an exponential increase of the full joint probability distribution (Moreira & Wichert, 2018).

Currently, quantum-like models are merely probabilistic and they cannot be used in decision-making settings, since decision-making implies the notion of utility. For instance, it is not enough for a doctor to know the probability of a patient having some disease. Rather, a doctor needs to act upon this information and decide what will be the best drug for the patient. At the heart of such a decision is the need to maximise the utility of the decision, which in this case equates to the decision that best promotes the well-being of the patient. Since current decision-making systems are based on classical probability theory, then they cannot capture and predict human paradoxical decisions, and instead of accommodating these deviations in human behaviour in the model, they are usually ignored and labelled as simply irrational, with the implication that they are "wrong".

In this sense, this paper aims to put together a comprehensive framework on how to describe the probabilistic nature of the human decision-making process with a focus on modelling optimal, sub-optimal and irrational (paradoxical) human decisions

by extending the previously proposed quantum-like Bayesian network (Moreira & Wichert, 2014, 2016a) to incorporate the notion of maximum expected utility. What distinguishes this work from the literature is the following: instead of proposing an alternative representation of the expected utility theory (like it is done in Mura, 2009), we retain expected utility as it is commonly understood, but we take advantage of the quantum interference terms produced in the quantum-like Bayesian Network to influence the probabilities used to compute the expected utility of some decision. In this way, we are not hypothesising a new type of expected utility. On the contrary, we propose incorporate standard expected utility as an extension of a probabilistic graphical model in the form of a compact graphical representation called an "influence diagram", which is simply a general graphical representation of the expected utility theory. The main difference is that instead of the utility function depending on classical probabilities, it will be influenced by probabilistic inferences computed by the quantum-like Bayesian network. Influence diagrams are probabilistic graphical models for decision-making that are widely used in the literature (for instance, in finance to determine the net present value of a project Lander & Shenoy, 2001, in economics to model antitrust enforcement Mortera, Vickard, & Vergari, 2013 or even in medical decision-making Owens, Shachter, & Robert F. Nease, 1997).

In this article, the utility-based influence diagram framework will be used to naturally explain the paradoxical findings of the prisoner dilemma game in regard to the expected utilities of the players. It is important to note that this research is not concerned with modelling the brain with quantum theory, nor is directly concerned with the idea that brain is a quantum computer (Busemeyer & Bruza, 2012). Instead, our model assumes that quantum wave functions are present in the macroscopic world, like it has been confirmed in a variety of scientific studies Amico, Fazio, Osterloh, & Vedral, 2008; Ghosh, Rosenbaum, Aepli, & Copper-smithl, 2003; Vedral, 2011. However, if such architecture had to be implemented, one can assume that the proposed quantum-like influence diagram is a theoretical assembly model that explains how stimuli represented by assemblies of neurons can be propagated during the decision process (Levine, 2009). This notion is inspired by the neural assembly theory introduced by Hebb (1949), where the author proposed a connection between the structures found in the nervous system and those involved in high-level cognition such as diagnostic problem solving. In our model an assembly may be in four states: (1) not activated since it is not working, (2) positively activated, (3) negative activated or (4) in a superposition state that is neither, positively activated or negatively activated. The connections between the assemblies correspond to the conditional probability values and are represented under the framework of probabilistic graphical models.

2. Background and fundamental concepts

The model proposed in this work is founded on probabilistic graphical models, namely on Bayesian networks, which are one of the most powerful structures known by the Computer Science community for deriving probabilistic inferences (for instance, in medical diagnosis, spam filtering, image segmentation, etc.) (Koller & Friedman, 2009). The main advantage of these models is that they provide a link between probability theory and graph theory. And a fundamental property of graph theory is its modularity: one can build a complex system by combining smaller and simpler parts. Computationally, it is easier to combine different pieces of evidence and to perform probabilistic inferences, instead of calculating all possible events and their respective beliefs in massive full joint probability distributions (Griffiths, Kemp, & Tenenbaum, 2008). In the same way,

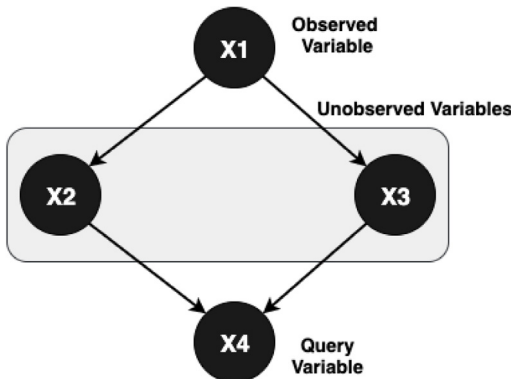


Fig. 1. Example of a classical Bayesian belief network.

Bayesian Networks represent the decision problem in small modules that can be combined to perform inferences (Pearl, 1988). Only the probabilities which are actually needed to perform the inferences are computed (Fig. 1).

This process can also be viewed under the perspective of human cognition (Griffiths et al., 2008). During the inference process, the decision-makers cannot process all possible information of the decision problem, and consequently, they combine several smaller pieces of evidence (or information) together with uncertainty about the decision problem in order to reach a final decision (Pearl, 1988). This lack of information can be translated into the feelings of ambiguity, uncertainty, vagueness, risk, ignorance, etc (Zadeh, 2006), and they are a consequence of various factors, such as limitations in their ability to observe the world, limitations in their ability to model it and possibly even because of innate nondeterminism (Koller & Friedman, 2009).

Under a classical point of view, uncertainty is represented by classical probability theory, where the decision-maker is assumed to be experiencing a definite state in each time period. Under a quantum probabilistic perspective, this representation of uncertainty is different. When reasoning under uncertainty, the decision-maker is in an indefinite state, which results in a superposition of beliefs (Busemeyer & Bruza, 2012). A superposition can be generally understood as the simultaneous occurrence of all the beliefs that the decision-maker is experiencing in a single time frame. This superposition of beliefs will result in the occurrence of quantum interference effects that under high levels of uncertainty can disturb the decision-maker's beliefs. One can look at quantum interference effects as waves that crash between each other, leading to waves (beliefs) that are destroyed (destructive interference) and waves that can be reinforced (constructive interference). This phenomena of quantum interference is also the core of quantum computation and the reason why such computers can achieve such high performances in terms of speed (Aaronson, 2013). Fig. 2 shows an example of the role of quantum interference effects within unobserved nodes in Bayesian networks.

2.1. Fundamental concepts in rationality and decision-making under the quantum-like approach

The main goal of the proposed quantum-like influence diagrams is to provide a unifying decision model for data-driven computational decisions, which are based on optimisation algorithms, and for human data-driven decisions, which are susceptible to cognitive biases. Under this framework, one can define different viewpoints on the notion of rationality, depending on the degrees of rationality that the decision-maker can experience.

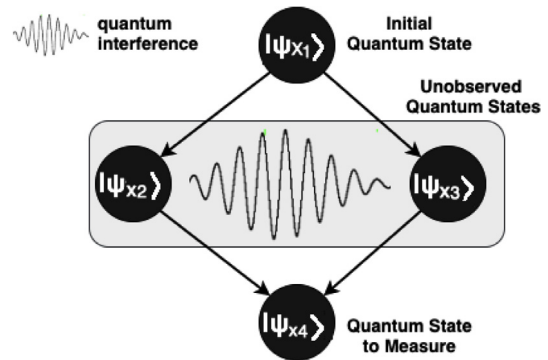


Fig. 2. Example of a quantum-like Bayesian belief network.

The views presented under the proposed quantum-like approach are similar to the one put forward by Gigerenzer and Goldstein (1996). They include decisions bounded in terms of time, processing power, information, etc. We extend this view to incorporate the notion of the *irrational mind*, a point in the decision-maker's belief space where heuristics are no longer sufficient to produce satisfying outcomes. Under the proposed quantum-like approach, we define the different views on rationality as it was proposed in the previous study of Moreira, Hammes, Kurdoglu, and Bruza (2020). Fig. 3 provides an illustration of these views.

- **Belief space:** Corresponds to the set of possible beliefs that are held by a decision-maker from the moment that (s)he is faced with a decision until (s)he actually makes the decision.
- **Unbounded Rationality:** Corresponds to the ideal scenario where the decision-maker has unbounded cognitive resources: unlimited time, unlimited processing power and unlimited information about the decision scenario. Note that these are optimal ideals that usually fall out from the reach of a human decision-maker, however computers can reach these states. Examples are the Maximum Expected Utility (von Neumann, 1996), Bayes rule (Pearl, 1988), likelihood maximisation (Kass & Wasserman, 1995), rules of Logic (Boole, 1847), etc.
- **Bounded Rationality:** Corresponds to the scenario where the decision-maker is bounded in terms of cognitive resources with limited information, time, and processing power. It is in these minds that the fast and frugal heuristics are applied (Kahneman, Slovic, & Tversky, 1982) and where decision-makers make sub-optimal decisions (i.e. decisions that lead to a positive utility).
- **Irrationality:** Corresponds to the bounded rational minds that are facing extremely high levels of uncertainty and for that reason, they lead to decisions with very poor performances in terms of an utility function. It is in this space that the fast and frugal heuristics start to fail and the decision-maker starts to experience cognitive dissonance effects, and starts to violate the rules of probability and logic. These types of decisions are hard to be captured by current decision support systems or current machine learning algorithms.

2.2. Bayesian networks

A Bayesian Network (BN) is a directed acyclic graph in which each node represents a random variable, and each edge represents a direct influence from the source node to the target node. The graph represents independence relationships between variables, and each node is associated with a conditional probability

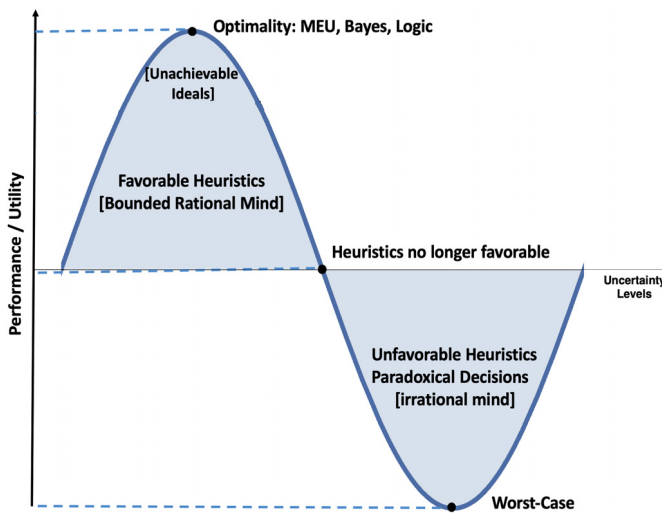


Fig. 3. Views on rationality under the quantum-like approach as proposed in Moreira, Hammes, et al. (2020).

table that specifies a distribution over the values of a node given each possible joint assignment of values of its parents (Pearl, 1988).

Bayesian networks can represent essentially any full joint probability distribution, which can be computed using the chain rule for Bayesian networks (Russel & Norvig, 2010). Let \mathcal{G} be a BN graph over the variables X_1, \dots, X_n . We say that a probability distribution, Pr , over the same space factorises according to \mathcal{G} , if Pr can be expressed as the product (Koller & Friedman, 2009)

$$Pr(X_1, \dots, X_n) = \prod_{i=1}^n Pr(X_i | Pa_{X_i}). \quad (1)$$

In Eq. (1), Pa_{X_i} corresponds to all the parent variables of X_i . The graph structure of the network, together with the associated factorisation of the joint distribution allows the probability distribution to be used effectively for inference (i.e. answering queries using the distribution as our model of the world). For some query Y and some observed variable e , the exact inference in Bayesian networks is given by Koller and Friedman (2009)

$$Pr(Y|E = e) = \alpha Pr(Y, e) = \alpha \sum_{w \in W} Pr(Y, e, w), \quad \text{with } \alpha = \frac{1}{\sum_{y \in Y} Pr(y, e)}. \quad (2)$$

Each instantiation of the expression $Pr(Y = y, e)$ can be computed by summing out all entries in the joint that correspond to assignments consistent with y and the evidence variable e . The random variable W corresponds to variables are neither query nor evidence. The α parameter corresponds to the normalisation factor for the distribution $Pr(Y, e)$ (Russel & Norvig, 2010). This normalisation factor comes from some assumptions that are made in Bayes rule (Russel & Norvig, 2010).

2.3. Quantum-like Bayesian networks

Moreira and Wichert (2014, 2016a) proposed a quantum-like Bayesian network which extends Bayesian networks by replacing probabilities by complex quantum probability amplitudes.

A quantum-like Bayesian network (QLBN) can be defined by a pair $(\mathcal{G}, \rho_{\mathcal{G}})$, where

- \mathcal{G} is a directed acyclic graph represented by a pair $\mathcal{G} = (V, E)$. Each vertex $v_i \in V$ is a random variable represented

by a quantum state in a complex Hilbert space $H_{\mathcal{G}}$, and $e_j \in E$ is a set of directed edges expressing relationships between vertices (Leifer & Poulin, 2008).

- $\rho_{\mathcal{G}}$ is a density operator in a composite state of independent complex Hilbert¹ spaces of different dimensions. The system $\rho_{\mathcal{G}}$ is defined over a fixed basis and therefore it satisfies the same conditional independence constraints as in a Bayesian network (Leifer & Poulin, 2008).

The next sections formalise the main elements of QLBNS by means of the Dirac notation (Appendix A presents the basic elements of this notation for the reader who is not familiar with it). Fig. 6 shows an example of a quantum-like Bayesian network. For details about the mathematical formalisms please refer to Appendix B.

State space

Let $H_{\mathcal{G}}$ be a complex Hilbert space that represents a quantum-like Bayesian network. Let $H_1 \in H_{\mathcal{G}}, H_2 \in H_{\mathcal{G}}, \dots, H_n \in H_{\mathcal{G}}$ be a set of different Hilbert spaces that makes up the QLBNS, then the Hilbert space $H_{\mathcal{G}}$ that represents the network is defined as the tensor product of each individual Hilbert space: $H_{\mathcal{G}} = H_1 \otimes H_2 \otimes \dots \otimes H_n$. The dimension of $H_{\mathcal{G}}$ corresponds to the size of the full joint probability distribution.

Quantum states

The random variables that make up the network are represented as quantum states. This means that random variables are represented as a probability distribution of complex probability amplitudes over the different outcomes that the random variable can have, instead of being specified as real numbers (like in the traditional Bayesian network).

In quantum-like Bayesian networks, one also needs to distinguish between two types of quantum states: (1) states corresponding to root nodes, and (2) states corresponding to child nodes.

Root nodes correspond to quantum pure states. In Fig. 2, the only root node that we have is the quantum state $|\psi_{X_1}\rangle$. An example of such state can be given by

$$|\psi_{X_1}\rangle = \alpha_0|0\rangle + \alpha_1|1\rangle, \text{ where } |\alpha_0|^2 + |\alpha_1|^2 = 1, \quad (3)$$

and the terms $|0\rangle$ and $|1\rangle$ are called basis states and correspond to the basis, $[1, 0]^T$ and $[0, 1]^T$, respectively. The variables α_0 and α_1 correspond to complex probability amplitudes of the form: $\sqrt{r}e^{i\theta}$, $r \in \mathbb{R}$.

Child nodes, on the other hand, represent a statistical distribution of different quantum states. This means that we represent child nodes as an ensemble where the conditioned probabilities can be found in one of the different quantum states in the ensemble (McMahon, 2007). We make this more concrete in the following example.

Fig. 4 shows the representation of a pure state (root node) and Fig. 5 shows the representation of an ensemble of states (child node). Note that, since quantum probability amplitudes are represented by complex numbers, one quantum state can be geometrically represented in different ways, according to the phase of the complex amplitude, θ .

Superposition state of a composite system

In quantum theory, all individual quantum states contained in a Hilbert Space are defined by a superposition state which

¹ A Hilbert space can be defined as a generalisation and extension of the Euclidean space into spaces with any finite or infinite number of dimensions. It is a vector space of complex numbers and offers the structure of an inner product to enable the measurement of angles and lengths (Hirvensalo, 2003).

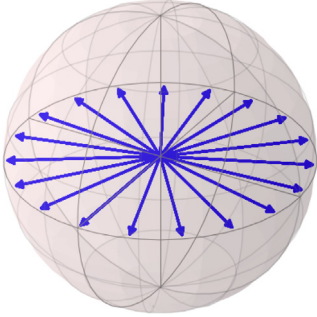


Fig. 4. Graphical representation of the pure state from Fig. 2, representing the configurations that the state $|\psi_1\rangle$ can have according to the quantum phase θ_1 and θ_2 , $|\psi_1\rangle = \alpha_0|0\rangle + \alpha_1|1\rangle$, with $\alpha_0, \alpha_1 \in \mathbb{R}$.

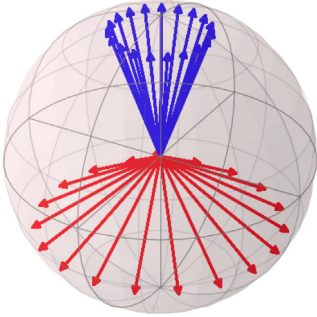


Fig. 5. Graphical representation of an ensemble of states from Fig. 2, representing the configurations that the state $|\psi_{X3}\rangle$ can have according to the parent state $|\psi_{X1}\rangle$.

is represented by a quantum state vector $|S\rangle$ comprising the occurrence of all events of the system. This can be analogous to the classical full joint probability distribution, with the difference that instead of using real numbers to express probabilities, one uses complex probability amplitudes.

In this sense, the superposition state $|S_G\rangle$ comprising all possible events in Hilbert space H_G is given by

$$|S_G\rangle = \sum_{k_1, k_2, \dots, k_n} \prod_{j \in G} \psi_{x=j|p_{a_{x=j}}} |k_1\rangle \otimes |k_2\rangle \otimes \dots \otimes |k_n\rangle, \quad (4)$$

where k_1, k_2, \dots, k_n corresponds to the basis of each quantum state in the network.

Density operator

The density operator, ρ_G , aims to describe a system where we can compute the probabilities of finding each state in the network. One way to achieve this is by computing a density operator through the outer product of the superposition state of the composite system, $|S_G\rangle$ (McMahon, 2007),

$$\rho_G = |S_G\rangle \langle S_G| = \begin{pmatrix} |\alpha_0|^2 & \alpha_0\alpha_1^* & \dots & \alpha_0\alpha_{n-1}^* \\ \alpha_1\alpha_0^* & |\alpha_1|^2 & \dots & \alpha_1\alpha_{n-1}^* \\ \vdots & \vdots & \ddots & \vdots \\ \alpha_{n-1}\alpha_0^* & \alpha_{n-1}\alpha_1^* & \dots & |\alpha_{n-1}|^2 \end{pmatrix},$$

$$\text{where } |\alpha_0|^2 + |\alpha_1|^2 + \dots + |\alpha_{n-1}|^2 = 1 \quad (5)$$

The density operator, ρ_G , corresponds to an $n \times n$ Hermitian matrix, where n is the number of quantum states in the network, that contains the *classical full joint probability distribution* of the network if we sum the elements of the *main diagonal*. In other

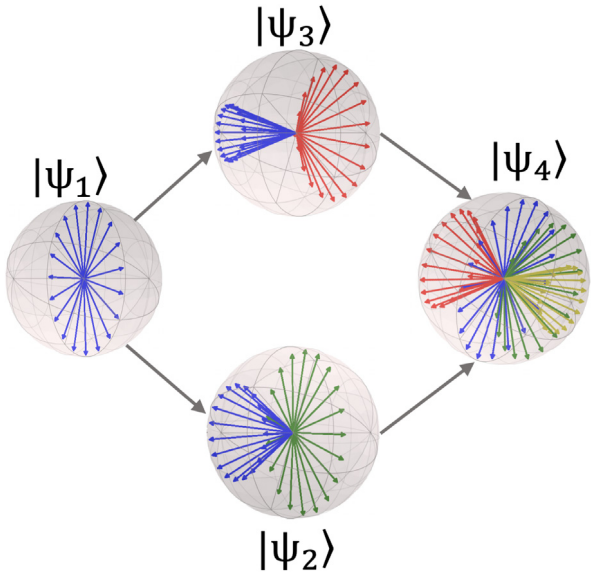


Fig. 6. General illustration of the quantum-like Bayesian network using quantum states instead of nodes.

words,

$$\text{Diag}(\rho_G) = \Pr(X_1, \dots, X_n) = \prod_{i=1}^n \Pr(X_i | P_{a_{X_i}}). \quad (6)$$

The density operator also contains quantum interference terms in the off-diagonal elements, which are the core of this model. It is precisely through these off-diagonal elements that, during the inference process, one is able to obtain quantum interference effects, and consequently, deviations from normative probabilistic inferences. It follows that this model allows different levels of representations of decisions under uncertainty ranging from (1) fully rational and optimal decisions (*fully classical*) that follow the axioms of expected utility (connected to rational theories of choice in Economics) (von Neumann & Morgenstern, 1953), (2) sub-optimal decisions that deviate from the predictions of expected utility theory, but still provide satisfying utilities to the decision-maker (connected to the theories of bounded rationality (Gigerenzer & Goldstein, 1996; Griffiths et al., 2008)), to (3) irrational decisions (Tversky & Shafir, 1992) (*fully quantum*) that reflect the choice of decisions that lead to lower utilities (connected to paradoxical decisions and cognitive bias). Note that quantum interference effects are non-linear functions that can be mapped to the non-linear activation functions in neural networks (Grossberg, 1988) (see Fig. 6).

Partial trace

During the inference process, it is necessary to trace out subgroup of quantum systems from the larger system, represented by the density operator ρ_G . In the example from Fig. 2, the system $\rho_G(X_1, X_2, X_3, X_4)$ represents the full network with the four states X_1, X_2, X_3, X_4 , in a 16×16 matrix,

$$\rho_{G(X_1, X_2, X_3, X_4)} = \begin{pmatrix} \alpha_{0,0} & \alpha_{0,1} & \alpha_{0,2} & \dots & \alpha_{0,15} \\ \alpha_{1,0} & \alpha_{1,1} & \alpha_{1,2} & \dots & \alpha_{1,15} \\ \alpha_{2,0} & \alpha_{2,1} & \alpha_{2,2} & \dots & \alpha_{2,15} \\ \vdots & \vdots & \vdots & \ddots & \vdots \\ \alpha_{15,0} & \alpha_{15,1} & \alpha_{15,2} & \dots & \alpha_{15,15} \end{pmatrix} \quad (7)$$

For many situations in Quantum Information Theory it is necessary to trace out a subgroup of quantum states from a larger

group. Given two quantum states ψ_X and ψ_Y , the general idea is to compute the average of the probability distribution of ψ_X over the information about ψ_Y (McMahon, 2007). This is performed by using the partial trace operator, which basically accesses certain positions of the density operator of the system, ρ_G , which is given by

$$\rho_{G(X)} = Tr_Y [\rho_{G(X,Y)}] \quad (8)$$

Computing probabilities

The final step of the quantum-like Bayesian network is to convert the complex probability amplitudes computed in the partial trace operation into real probability values. This operation is dependent on the query that the decision-maker asks. In order to compute the probability of some query $X = i$, one needs an operator to select all the entries of the density operator ρ_G that satisfy the assignment i of query, X . This is the same operation as in exact probabilistic inference, where one selects the entries of the full joint distribution that match the query assignments. In this sense, we can define the operator M as a $1 \times N$ column vector with zeros in all positions, except in the ones that satisfy the assignment index, i , of the query. We denote this as $\mathbb{1}_{X=i}$. Therefore, the probability of a variable X_i , given some evidence variable, e , is given by,

$$Pr(X = i|e) = \langle M | Tr_Y[\rho_{G(X,Y)}] | M \rangle \quad \text{where } |M\rangle = \mathbb{1}_{X=i} \quad (9)$$

Since we are considering a fixed basis in our system, the partial trace over the density operator ρ_G , can be simplified to Eq. (10). The summation is over all possible y , i.e. all possible combinations of values of the unobserved values y of variable Y . The term γ corresponds to a normalisation factor. Since the conditional probability tables used in Bayesian networks are not unitary operators with the constraint of double stochasticity (like it is required in other works of the literature Busemeyer et al., 2006; Pothos & Busemeyer, 2009), we need to normalise the final scores. In classical Bayesian inference, on the other hand, normalisation is performed due to the independence assumption made in Bayes rule

$$Pr(X|e) = \gamma \left| \sum_y \prod_{k=1}^N \psi(X_k|Parents(X_k), e, y) \right|^2 \quad (10)$$

Note that double stochasticity of a square matrix requires that each row and each column of non-negative real numbers adds up to one. Expanding Eq. (10) will lead to the quantum-like marginalisation formula (Moreira & Wichert, 2014), which is composed of two parts: one representing the classical probability and the other representing the interference term (which corresponds to the emergence of destructive/constructive interference effects)

$$\begin{aligned} Pr(X|e) &= \gamma \sum_{i=1}^{|Y|} \left| \prod_k \psi(X_k|Pa_{X_k}, e, y = i) \right|^2 + 2\text{Interference} \\ \text{Interference} &= \sum_{i=1}^{|Y|-1} \sum_{j=i+1}^{|Y|} \left| \prod_k \psi(X_k|Pa_{X_k}, e, y = i) \right| \\ &\quad \times \left| \prod_k \psi(X_k|Pa_{X_k}, e, y = j) \right| \cos(\theta_i - \theta_j) \end{aligned} \quad (11)$$

Note that, in Eq. (11), if one sets $(\theta_i - \theta_j)$ to $\pi/2$, then $\cos(\theta_i - \theta_j) = 0$. This means that the interference term is cancelled and the quantum-like Bayesian network collapses to its classical counterpart. In other words, one can see the quantum-like Bayesian

Network as a more general and abstract model of the classical network, since it represents both classical and quantum-like behaviour. Setting the angles to right angles means that all cosine similarities are either 0 or 1, transforming a continuous-valued system to a Boolean-valued system. Moreover, if the Bayesian network has N binary random variables, we will end up with 2^N free θ parameters, which is the size of the full joint probability distribution.

Summary

To conclude this section, in Table 1, we present the main differences between the representation of the quantum-like Bayesian network and its classical counterpart. Although most operations that comprise the QLBN have a direct mapping from the BN, the core difference between them is concerned with the joint distribution and, consequently, with the marginalisation process. By representing belief states as complex quantum probability amplitudes in a complex Hilbert space, we are able to get the representation of the full joint distribution of the network by using a density operator, ρ_G . The off-diagonal elements of this operator correspond to quantum interference effects that will enable deviations from normative probabilistic inferences which are obtained in traditional BNs. During the partial trace, one is able to select the subsystem of the density operator that corresponds to the variable being queries, together with other information about other variables in the network.

These quantum interference effects are the core of the QLBN and are the result of the interferences caused by the quantum wave function. As shown in Vedral (2011), although we are in a full Newtonian world, there is growing evidence that the wave function and other quantum effects can manifest in the macroscopic world (see Amico et al., 2008; Ghosh et al., 2003). For instance, European robins are little birds that have some particles in their eyes that interact and become entangled with Earth's magnetic field, allowing the birds to have a compass for their migration route (Vedral, 2011).

The current work takes a similar position. We assume that decision-makers (either people within human cognitive tasks, or machines in general decision-making problems) can be affected by the wave function while reasoning in decision-scenarios with high levels of uncertainty. This wave function can provide interference effects in different levels, and lead to deviations from normative probabilistic inferences. This is why we refer to the model as *quantum-like*, instead of a pure quantum system that would require a microscopic, particle world.

2.4. Setting interference terms: The law of balance

So far, we presented a general model, which allows different levels of probabilistic reasoning in decision scenarios, ranging from normative and rational inferences, to sub-optimal, or even irrational, inferences. In this section, we will address the hard problem of how to find the right quantum interference terms that can express the different types of human decisions, namely optimal rational decisions, sub-optimal decisions and irrational decisions. In the recent works of Moreira and Wichert (2016a) and Wichert and Moreira (2018), the authors proposed two methods to automatically set quantum interference terms to accommodate and predict human paradoxical decisions. These methods are the *dynamic similarity heuristic* (Moreira & Wichert, 2016a) and the *law of balance* (Wichert & Moreira, 2018). Both methods seemed to be specially effective in predicting violations of the Sure Thing Principle (Savage, 1954; Tversky & Shafir, 1992), although some recent studies show a potential application

Table 1

Main differences between the quantum-like Bayesian network (Moreira & Wichert, 2014, 2016a) and the traditional Bayesian network (Pearl, 1988).

Quantum-like bayesian network		
Description	Representation	Description
Belief State	\vec{x}	$ \psi_x\rangle$
Conditional states	$Pr(\vec{x} \vec{y})$	$ \psi_{y x}\rangle = [\psi_{y x=0}; \psi_{y x=1}]$
Joint distribution	$\vec{x} \otimes \vec{y}$	$\hat{\rho} = \sum \psi_x \otimes \psi_y\rangle \langle \sum \psi_x \otimes \psi_y $
Marginalisation	$\vec{x} = \sum_y \vec{x} \otimes \vec{y}$	$\hat{\rho}_x = Tr_Y(\hat{\rho}_{XY})$
Inference	$Pr(X = i e)$	$Pr(X = i e) = \langle M Tr_Y[\rho_{G(X,Y)}] M \rangle$

$$Pr(B) = \alpha [\sum_{i=1}^N |\psi_i|^2 + 2 \cdot |\psi_1| \cdot |\psi_2| \cdot \cos(\theta_1 - \theta_2) + 2 \cdot |\psi_1| \cdot |\psi_3| \cdot \cos(\theta_1 - \theta_3) + \dots]$$



Fig. 7. Example of how to compute the similarity heuristic as it was proposed in Moreira and Wichert (2016a).

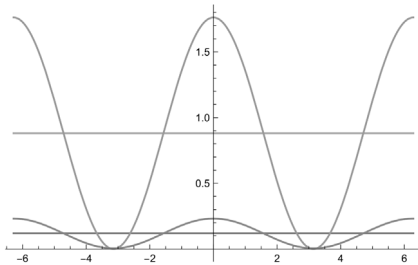


Fig. 8. Example of an intensity wave where one of the quantum interference waves completely dominates the other.

of the dynamic similarity heuristic within a real-world credit application problem (Moreira et al., 2018).

2.4.1. The similarity heuristic

In the Similarity Heuristic, the interference parameters θ are obtained by extracting the similarity values between the marginal distribution vectors (Fig. 7). This is achieved by computing the cosine similarity between them, which is a widely used similarity function in information retrieval (Baeza-Yates & Ribeiro-Neto, 2010). The cosine similarity will provide three degrees of similarity between the belief vectors during the inference process and will allow the extraction of information that can be used to compute the quantum interference terms. For details on how to compute the similarity heuristic, the reader can refer to the original work from Moreira and Wichert (2016a) for more theoretical and technical clarifications.

2.4.2. The law of balance

One important element in quantum-like Bayesian networks is concerned with the normalisation factor that is used during probabilistic inference. While in traditional Bayesian networks this normalisation factor derives from the notions of conditional independence and Bayes rule, within a quantum-like formalism this is not clear since the quantum interference terms are also present in the normalisation process. This turns the representation of the quantum waves skewed and more sensitive to changes in the quantum interference terms.

In Wichert and Moreira (2018), the authors proposed a balanced quantum-like Bayesian network in which the normalisation process occurs by taking dominant quantum interference

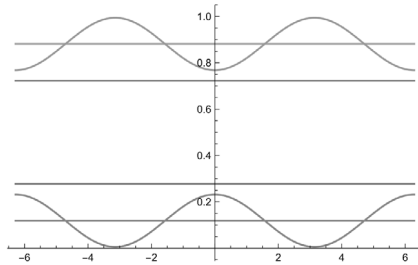


Fig. 9. Example of the outcome of the application of the Law of Balance in order to make the dominant and the less representative wave fluctuate around their classical probability values with similar amplitudes, so they can cancel each other upon Bayes normalisation (Wichert & Moreira, 2018).

waves and balancing them in such a way that, when Bayes normalisation is being applied upon probabilistic inferences, they cancel each other out. This notion of balancing the quantum interference waves is represented in Figs. 8 and 9, where one can see that a dominant and an under representative quantum interference wave are balanced and are modelled in a way that allows them to fluctuate around their classical predictions. The quantum interference is predicted by choosing the wave that has led to the highest uncertainty, in other words, the wave that has the highest entropy. For more details about the law of balance, please refer to Wichert and Moreira (2018).

3. Influence diagrams

Generally speaking, an “influence diagram”, \mathcal{I} , is a compact graphical representation of a decision scenario. An example of an influence graph is presented in Fig. 12, where $X_1, \dots, X_n \in \mathcal{X}$ represent random variables (nodes) of a Bayesian Network. \mathcal{D} represents a decision, and U denotes the utility function. The goal of an influence graph is to make a decision \mathcal{D} maximise the Expected Utility function U by taking into account probabilistic inferences performed in the Bayesian Network (Koller & Friedman, 2009).

An Influence Graph is a directed acyclic graph with three kinds of nodes:

- **Random Variables:** A random variable is usually denoted $X_1, \dots, X_n \in \mathcal{X}$. Each node belongs to a Bayesian Network and is followed by a conditional probability distribution table that expresses the probability distribution of

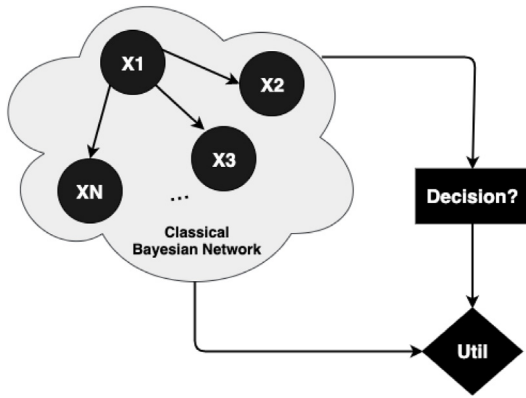


Fig. 10. General structure of an influence diagram, containing a Bayesian network with random variables, X_1, X_2, \dots, X_n , a Decision node, \mathcal{D} , and an Utility node, U .

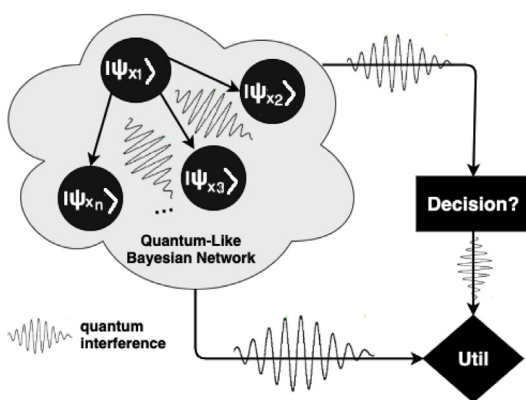


Fig. 11. General structure of a quantum-like influence diagram, containing a quantum-like Bayesian network where each node is a quantum state $|\psi_{x_1}\rangle, \dots, |\psi_{x_n}\rangle$, a Decision node, \mathcal{D} , and an Utility node, U . Quantum interference effects can influence the maximum expected utility of some decision D .

a node given its parents' nodes, $Pr(X|Pa_X)$. In Fig. 10, this corresponds to the oval shape nodes.

- **Decision Nodes:** A decision node \mathcal{D} that is also known as the decision rule. The decision rule is represented by a deterministic conditional probability distribution that assigns probability 1 to a single action for each joint assignment of the parents of \mathcal{D} , with zeros for all other actions. In a decision scenario, this could correspond to an individual's decision: gamble/not gamble, invest/not invest, perform surgery/not perform surgery, etc. In Fig. 10, this corresponds to the rectangular shape.
- **Utility Nodes:** The utility node $U \in \mathcal{U}$ never has child nodes (contrary to Random Variables and Decision nodes). Utility nodes are followed by utility factors that map each possible joint assignment of their parents into an utility value.

3.1. Maximum expected utility in influence diagrams

Given a set of possible decision rules, δ_A , the goal of an Influence Diagrams is to compute the decision rule that leads to the Maximum Expected Utility in relation to decision D .

Additionally, $Pr_{\delta_A}(x|a)$ corresponds to a full joint probability distribution of all possible outcomes, x , given different actions a belonging to the decision rules δ_A . This can be expressed in the

Expected Utility formula for some decision, D , as

$$EU[\mathcal{D}[\delta_A]] = \sum_{x,a} Pr_{\delta_A}(x,a) U(x,a). \quad (12)$$

The goal is to choose some action a that maximises the expected utility with respect to some decision rule, δ_A :

$$a^* = \operatorname{argmax}_{\delta_A} EU[\mathcal{D}[\delta_A]] \quad (13)$$

One can map the expected utility formalism of Bayesian networks in the following way. Knowing that $Pr_{\delta_A}(x|a)$ corresponds to a full joint probability distribution of all possible outcomes, x , given different actions a belonging to the decision rules δ_A . This allows the full joint probability distribution to be factorised using the chain rule:

$$EU[\mathcal{D}[\delta_A]] = \sum_{x,a} Pr_{\delta_A}(x,a) U(x,a) \quad (14)$$

$$EU[\mathcal{D}[\delta_A]] = \sum_{x_1, \dots, x_n, A} \left(\left(\prod_i Pr(X_i|Pa_{X_i}) \right) U(Pa_U) \delta_A(A|Z) \right) \quad (15)$$

In Eq. (15), $Z = Pa_A$ represents the parent nodes of action A . We can factorise Eq. (15) in terms of the decision rule, δ_A , obtaining

$$EU[\mathcal{D}[\delta_A]] = \sum_{Z,A} \delta_A(A|Z) \left(\sum_W \left(\prod_i Pr(X_i|Pa_{X_i}) \right) U(Pa_U) \right), \quad (16)$$

where $W = \{X_1, \dots, X_n\} - Z$ corresponds to all nodes of the Bayesian network that are not contained in the set of nodes in Z .

By marginalising the summation over W , we obtain an expected utility formula that is written only in terms of the factor $\mu(A, Z)$. Note that this factor corresponds to a joint between random variable Z (the outcomes of some action a) and action a , and contains information about the utility of each action

$$EU[\mathcal{D}[\delta_A]] = \sum_{Z,A} \delta_A(A|Z) \mu(A, Z) \quad (17)$$

The Maximum Expected Utility for an Influence Diagrams is given by Koller and Friedman (2009):

$$\delta_A^*(a, Z) = \alpha(x) = \begin{cases} 1 & a = \operatorname{argmax}(A, Z) \\ 0 & \text{otherwise} \end{cases} \quad (18)$$

The influence diagrams presented, since they make use of Bayesian networks, they cannot express decisions that are either sub-optimal or paradoxical. In the next section, we present an extension of the influence diagrams within a quantum-like framework in order to describe the probabilistic nature of the decision-making process with a focus on modelling optimal, sub-optimal and irrational (paradoxical) human decisions by using the formalisms of quantum-like Bayesian networks together with the notion of maximum expected utility. Instead of proposing an alternative representation of the expected utility theory, we retain expected utility as it is commonly understood within an influence diagram representation, but we take advantage of the quantum interference terms produced in the quantum-like Bayesian Network to influence the probabilities used to compute the expected utility of some decision.

4. Quantum-like influence diagrams

The proposed quantum-like influence diagram is built upon the formalism of quantum-like Bayesian networks presented in

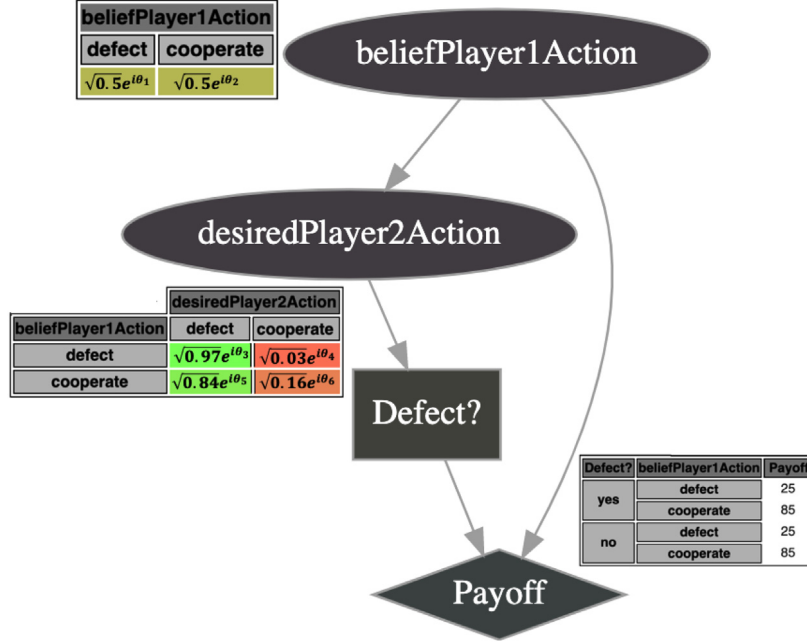


Fig. 12. Influence diagram representation of the Prisoner's Dilemma experiment performed by Tversky and Shafir (1992). In this model, the utility node corresponds to the payoff matrices that were used throughout the different experiments conducted in the literature.

Section 2.3, where classical probabilistic inferences are replaced by quantum-like inferences.

In order to derive the full mathematical formalism of $EU[\mathcal{D}[\delta_A]]$, we will start by considering a simple decision scenario with two random variables, X_1 and X_2 , and later generalise for the case of N variables. The classical $EU[D[\delta_A]]$ for these two random variables is

$$EU[\mathcal{D}[\delta_D]] = \sum_{X_1, X_2, A} Pr(X_1)Pr(X_2|X_1)U(X_1, D)\delta_D(D|X_2). \quad (19)$$

For the quantum counterpart of Eq. (19), one can represent the probabilities of the random variables X_1 and X_2 as a quantum superposition $|S_G\rangle$, which belongs to the quantum system \mathcal{G} ,

$$|S_G\rangle = \sum_{i_1} \sum_{i_2} \prod_{j \in G} \psi_{Xj|Pa_{Xj}} |i_1\rangle \otimes |i_2\rangle$$

This superposition state can describe the full joint distribution of the system by computing the density operator, $\rho_{\mathcal{G}}(X_1, X_2)$,

$$\rho_{\mathcal{G}(X_1, X_2)} = |S_G\rangle \langle S_G|.$$

Since the density operator, $\rho_{\mathcal{G}(X_1, X_2)}$, represents the full joint probability distribution of the system, then one can replace the classical joint probability term $Pr(X_1)Pr(X_2|X_1)$ of Eq. (19) by the quantum counterpart, as

$$EU[\mathcal{D}[\delta_D]] = \sum_D \rho_{\mathcal{G}} U(Pa_U) \delta_D(D|Z) \quad \text{where } Z = Pa_D. \quad (20)$$

One can rewrite Eq. (23) by a set of factors. For this, one needs to marginalise out variable X_1 . In a classical setting, this would be

$$EU[\mathcal{D}[\delta_A]] = \sum_{A, Z} \delta_D(D|X_2) \sum_w Pr(X_1)Pr(X_2|X_1)U(X_1, D)$$

$$\text{where } W = \{X_1, X_2\} - Z. \quad (21)$$

This marginalisation process in the quantum system \mathcal{G} corresponds to the partial trace operation $\rho_{\mathcal{G}(X_2)} = Tr_{X_1} \rho_{\mathcal{G}(X_1, X_2)}$. By replacing the classical term $\sum_w Pr(X_1)Pr(X_2|X_1)$ in Eq. (21) by its

quantum counterpart, one can obtain,

$$EU[\mathcal{D}[\delta_D]] = \sum_{D, X_2} \delta_D(D|X_2) \rho_{\mathcal{G}(X_2)} U(Pa_U) \quad (22)$$

The term $\rho_{\mathcal{G}(X_2)} U(Pa_U)$ will generate both a classical probabilistic inference and a quantum interference term, like it was presented in Eq. (11) in Section 2.3. This means that this partial trace operation will be dependent on the quantum interference parameter phase θ , which represents the degree of uncertainty of the decision-maker towards the decision scenario D . Just like in the classical counterpart, one can rewrite the term $\rho_{\mathcal{G}(X_2)} U(Pa_U)$ as an utility factor λ that depends not only the decision D , but also on the uncertainty values represented by quantum interference, $\lambda(D, X_2 : \theta_{X_1, X_2})$,

$$EU[\mathcal{D}[\delta_D]] = \sum_{D, X_2} \delta_D(D|X_2) \lambda(D, X_2 : \theta_{X_1, X_2}). \quad (23)$$

For a quantum-like Bayesian network with N quantum systems, the general formula for the maximum expected utility in influence diagrams is given by

$$EU[\mathcal{D}[\delta_A]] = \sum_{Z, A} \delta_A(A|Z) \lambda(A, Z : \Theta) \quad (24)$$

$$\delta_A^*(a, Z) = \alpha(x) = \begin{cases} 1 & a = \text{argmax } \lambda(A, Z : \Theta) \\ 0 & \text{otherwise} \end{cases} \quad (25)$$

In the next, we will show how to apply the formalisms of quantum-like influence diagrams in different experiments of the literature reporting violations in the law of total probability and paradoxical human decisions under uncertainty.

5. Quantum-like inferences in paradoxical decision scenarios: the case of the Prisoner's Dilemma

In this paper, we apply the formalism of the quantum-like influence diagrams in order to analyse and predict human paradoxical decisions that have been reported throughout the literature, namely in experiments concerned with violations to the

Sure Thing Principle under the Prisoner's Dilemma game (Tversky & Shafir, 1992).

The Sure Thing Principle (Savage, 1954) is a fundamental principle in economics and probability theory and states that if one prefers action A over B under state of the world X , and if one also prefers A over B under the complementary state of the world, $\neg X$, then one should always prefer action A over B even when the state of the world is unspecified. Several experiments have shown that people violate this principle in decisions under uncertainty, leading to paradoxical results and violations of the classical law of total probability (Aerts, Broekaert, & Smets, 2004; Birnbaum, 2008; Tversky & Kahneman, 1974, 1983; Tversky & Shafir, 1992). The prisoner's dilemma is an example where, under uncertainty, people violate the sure thing principle, by being more cooperative in decisions under uncertainty.

The prisoner's dilemma game can be summarised as follows. There are two prisoners who are in separate solitary confinements with no means of speaking to or exchanging messages with the other. The police offer each prisoner an agreement: each prisoner is given the opportunity either to betray the other (Defect), by testifying that the other committed the crime, or to Cooperate with the other by remaining silent.

In order to test the veracity of the Sure Thing Principle under the Prisoner's Dilemma game, experiments were made in where three conditions were tested:

- Participants were informed that the other participant chose to *Defect* (**Condition 1**: Known to defect);
- Participants were informed that the other participant chose to *Cooperate* (**Condition 2**: Known to cooperate);
- Participants had *no information* about the other participant's decision (**Condition 3** : Unknown).

Table 2 summarises the results of these experiments for the three conditions. The column classical prediction shows the classical probability of a player choosing to *Defect*, given that the decision of Player 1 is unknown (Condition 3).

Each one of the experiments in **Table 2** was executed using a different payoff matrix. **Table 3** summarises all the payoff matrices that were used in each experiment.

The concept of human behaviour deviating from the predictions of expected utility theory is not something new. There are many studies suggesting that humans tend to deviate from optimal Bayesian decisions (Bowers & Davis, 2011), which is not consistent with expected utility theory. Many approaches have been proposed in the literature in order to overcome these limitations. For instance, recently Peters (2019) criticised the notion of expected utility by showing that it is built under false assumptions, and proposed the concept of ergodicity economics as an alternative model to optimise time-average growth rates. Another work from Schwartzenbeck et al. (2015) describes irrational behaviour as a characteristic of suboptimal behaviour of specific groups (Beck, Ma, Pitkow, Latham, & Pouget, 2012). Their main argument is to look at irrational behaviour as a subject-specific generative model of a task, as opposed of having a single optimal model of behaviour (like it is predicted by expected utility theory).

In the next section, we use each payoff matrix as the utility node of the proposed quantum-like influence diagram and we will analyse the impact of quantum-like probabilistic inferences in the computation of the Maximum Expected Utility, in order to accommodate the paradoxical results observed in Condition 3 of the experimental findings of Li and Taplin (2002) and Tversky and Shafir (1992). Specific information about the model executions of these experiments and details about the mathematical framework used, will be publicly available in the QuLBiT (Quantum-Like

Bayesian inference Technologies) (Moreira, Hammes, et al., 2020) repository.²

5.1. Representation of the influence diagram

We used the values from Conditions 1 and 2 of the Prisoner's Dilemma game experiment reported in the literature to model the quantum-like Bayesian network of the influence diagram, and we used the game's correspondent payoff matrix as the utility node. We modelled the Prisoner's Dilemma experiment with two random variables with respect to the cognitive point of view of Player2.

- **Belief Player1 Action:** is a random variable representing the personal beliefs that Player 2 has regarding the action that his opponent (Player 1) might choose. These personal beliefs can be modelled as prior probabilities representing Player 2 full uncertainty towards Player 1's decisions. Beliefs represent the state of the decision-maker with respect to his opponent. This recognises that what the decision-maker believes about his opponent's decisions may not necessarily be true (and in fact may change in the future). In our experiments, given that no prior information is given to the player during condition 3, we will assume neutral priors. We will assume that the decision-maker believes that his opponent has an equal chance of either choosing to *defect* or to *cooperate*.
- **Desired Player 2 Action:** is a random variable representing the decision-maker's motivational state. They represent objectives or situations that the decision-maker would like to accomplish or bring about. In this case, it will be either to *cooperate* or to *defect* according to the goal of the decision-maker: a more cooperative strategy or a more selfish strategy.

Fig. 12 shows a quantum-like influence diagram representing the experiments conducted by Tversky and Shafir (1992). For each experiment reported in **Table 2**, we created and analysed a quantum-like influence diagram.

5.2. Analysis of quantum-like probability distributions

In this section, we analyse the probabilistic inferences of the Quantum-Like Bayesian networks to accommodate the decision-maker's reasoning process together with the impacts of the non-linearity of quantum interference terms as non-linear functions for probabilistic reasoning under uncertainty. For simplicity, we will denote node *Belief Player1 Action* as $P1$ and node *Desired Player 2 Action* as $P2$. A detailed step-by-step application of the quantum-like influence diagrams to Shafir and Tversky (1992) can be found in Appendix B. The maximum expected utility of this experiment computed with the proposed quantum-like influence diagram is illustrated in **Fig. 13**.

From the quantum-like probabilistic inference, a set of quantum interference terms emerge, θ_{def} and θ_{coop} , that will introduce a non-linearity in the reasoning process and that will be able to express three types of decisions under uncertainty: (1) fully rational and optimal decisions that follow the axioms of expected utility (connected to rational theories of choice in Economics), (2) sub-optimal decisions that deviate from the predictions of expected utility theory (connected to the theories of bounded rationality (Griffiths et al., 2008)), and (3) irrational decisions that reflect the choice of utilities that lead to the minimum utility (connected to paradoxical decisions).

² <https://git.io/Je1y2>

Table 2

Different experiments of the prisoner's dilemma game where the goal is to find violations to the Sure Thing principle. The entries of the table that are highlighted correspond to experimental settings where there was not verified a violation to the Sure thing principle. Each experiment used a different payoff matrix.

Experiments in Literature	Player 1 Known to defect	Player 1 Known to cooperate	Player 1 Unknown decision	Classical prediction Prob. prediction
Tversky and Shafir (1992)	0.9700	0.8400	0.6300	0.9050
Li and Taplin (2002) Game 1	0.8200	0.7700	0.7200	0.7950
Li and Taplin (2002) Game 2	0.7333	0.6670	0.6000	0.7000
Li and Taplin (2002) Game 3	0.8000	0.7667	0.6300	0.7833
Li and Taplin (2002) Game 4	0.9000	0.8667	0.8667	0.8834
Li and Taplin (2002) Game 5	0.8333	0.8000	0.7000	0.8167
Li and Taplin (2002) Game 6	0.7667	0.8333	0.8000	0.8000
Li and Taplin (2002) Game 7	0.8667	0.7333	0.7667	0.8000

Table 3

Payoff matrices used in each experiment of the Prisoner's Dilemma of the literature. In the payoffs, d corresponds to defect and c to cooperate. The first payoff corresponds to player 1 and the second to player 2, so the payoff entry dc means that player 1 chooses defect and player 2 chooses cooperate.

Shafir and Tversky (1992)		Li and Taplin (2002)																	
		Game 1		Game 2		Game 3		Game 4		Game 5		Game 6		Game 7					
Payoff		dd	dc	30	25	30	25	73	25	30	25	80	78	43	10	30	10	30	10
cd		85	75	85	75	85	75	85	36	85	83	85	46	60	33	60	33	60	33

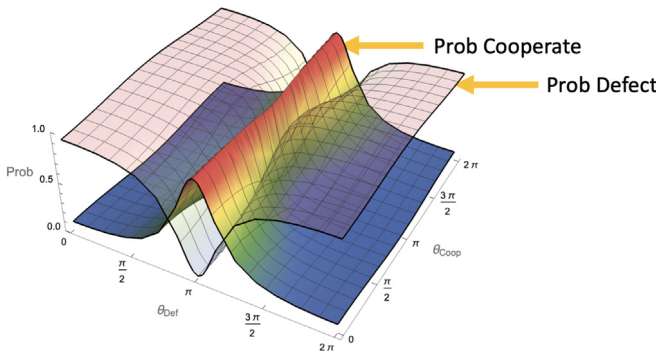


Fig. 13. Evolution of quantum interferences using quantum-like probabilistic inferences together with Bayes normalisation rule over Feynman's path diagrams (Moreira & Wichert, 2014, 2016a).

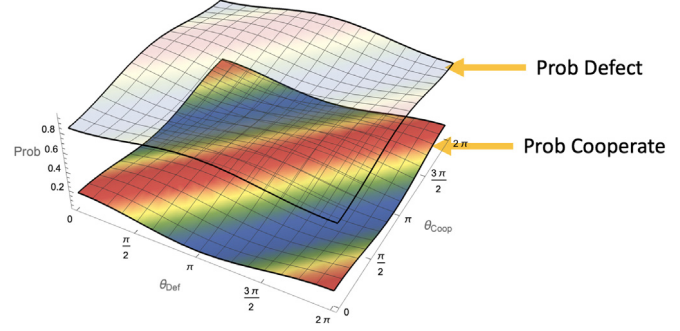


Fig. 14. Evolution of quantum interferences using quantum-like probabilistic inferences together with the Law of Balance (Wichert and Moreira, 2018) for normalisation.

One can analyse how the decision-maker's probabilistic inferences change according to the uncertainty levels represented by the quantum interference terms θ_{coop} and θ_{def} , which represent the belief of the player in choosing a cooperate strategy or a defect strategy, respectively. Fig. 13 shows these probabilistic inferences using Bayes normalisation rule over Feynman's path diagrams (Moreira & Wichert, 2014, 2016a), and Fig. 14 shows these probabilistic inferences using the law of balance (Wichert & Moreira, 2018).

The Law of Balance (Wichert & Moreira, 2018) and the Dynamic Similarity Heuristic (Moreira & Wichert, 2016a) provide a mathematical formalism to find the values for the quantum interference parameters θ_{def} and θ_{coop} that predict the paradoxical findings concerned with violations to the Sure Thing Principle. The results of the quantum interference parameters, together with their probabilistic predictions across all experiments reported in Table 2 can be found in Table 4 (see Fig. 15). Fig. 15 shows the impact of the quantum interference terms using the law of balance and Bayes normalisation.

Table 4 shows that the quantum-like Bayesian network was able to accommodate the paradoxical outcomes found in different experiments of the literature with respect to the Prisoner's dilemma game, while classical probability inference was not. Table 4 also shows that, the similarity heuristic was able to perform good approximations to the data. However, due to

the normalisation of the waves, these waves become skewed and the quantum interference parameters become very sensitive to small changes, leading to overestimations and underestimations in the prediction of the probability values (Fig. 13). That is, a small change in a quantum interference parameter will lead to a completely different probability value, which resembles the notion of deterministic chaos, where small differences in initial conditions yield widely diverging outcomes in a system.

With the law of balance on the hand, we observe a different scenario. Since the interference of the waves cancel each other during Bayesian inference, then these waves are not skewed and they provide a more uniform distribution for the quantum interference terms, which makes them less susceptible for the problems caused by deterministic chaos (Fig. 14). However, in terms of fitting the experimental findings in the literature, their performance slightly drops.

In terms of the probabilistic inferences of the quantum-like Bayesian network, it seems that quantum interference effects can accommodate and predict the irrational decisions of the decision-maker. However, in terms of decision-making, probability distributions are not enough. In medical decision-making, for instance, it is not enough for a doctor to know the probability of a patient having a disease. The doctor needs to take action,

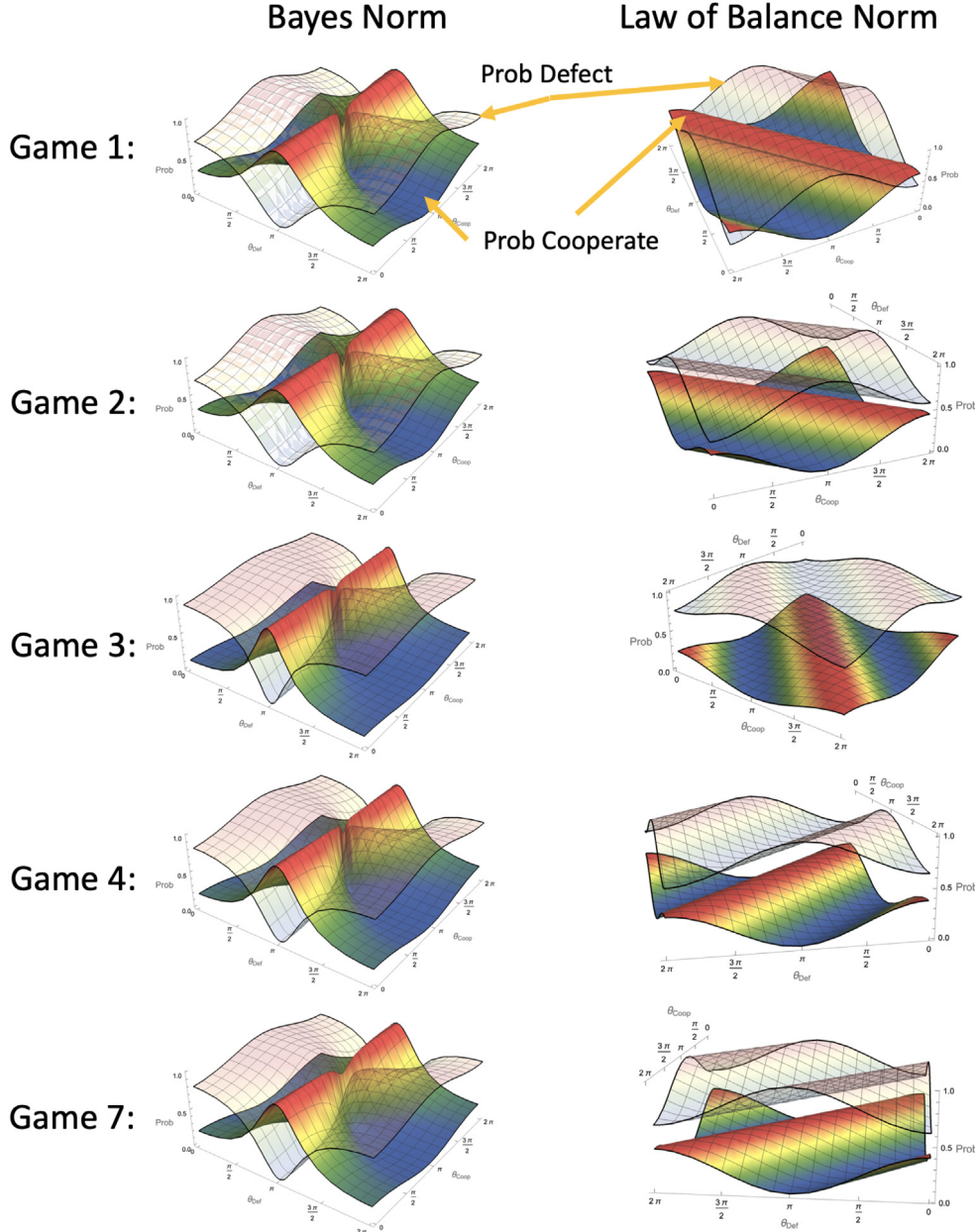


Fig. 15. Impact of quantum interference terms in Player 2 probabilistic inferences in Li and Taplin (2002) experiments. Note that the quantum interference terms represent the degree of uncertainty of the player. The different quantum interference terms can show higher probabilities of the player making a fully rational decision, a sub-optimal decision and a total irrational decision.

Table 4

Quantum-like probabilistic inferences over condition 3 for each experiment reported in Table 2, using the predictions computed using the Law of Balance (LD: $Pr(\text{Defect})$) and the Dynamic Similarity Heuristic with Bayes normalisation (Bayes Norm: $Pr(\text{Defect})$).

Literature	Pr(Defect) Condition 3	LB: Pr(Defect)	Bayes Norm: Pr(Defect)	LB Norm Error (%)	Bayes Norm Error (%)
Shafir and Tversky (1992)	0.6300	0.8357	0.6408	20.57	1.08
Li and Taplin (2002) Game 1	0.6000	0.5915	0.6313	0.847	3.13
Li and Taplin (2002) Game 2	0.6300	0.4018	0.7011	22.8179	7.11
Li and Taplin (2002) Game 3	0.8667	0.5673	0.8113	29.9359	5.54
Li and Taplin (2002) Game 4	0.7000	0.7679	0.7341	6.7894	3.41
Li and Taplin (2002) Game 5	0.7000	0.6341	0.7006	6.5942	0.06
Li and Taplin (2002) Game 6	0.8000	0.6028	0.7169	19.7208	8.31
Li and Taplin (2002) Game 7	0.7667	0.6115	0.7159	15.525	5.08

based on this uncertainty and see which treatments would be the best for the patient (treatments that maximise the utility of the

patient). In this sense, in the next section, we analyse the maximum expected utility within the quantum-like paradigm, where

the utilities of the player are influenced by quantum interference effects.

5.3. Analysis of the maximum expected utility in quantum-like influence diagrams

In this section, we validate the outcomes in terms of maximum expected utility of the proposed quantum-like influence diagrams for each experiment of the Prisoner's Dilemma game reported in [Table 2](#). We computed the Maximum Expected Utility (MEU) in two different ways: (1) using the law of balance together with the law of maximum entropy ([Wichert & Moreira, 2018](#)), and (2) the Bayes normalisation over Feynman's path diagrams using the similarity heuristic ([Moreira & Wichert, 2014, 2016a](#)). We applied the same values of the quantum interference parameters that we used to compute the probabilistic inferences of the quantum-like Bayesian network as reported in [Table 4](#). [Table 5](#) presents the results obtained.

Before discussing the results, it is important to note that the Prisoner's Dilemma game has a *strictly dominant strategy* which is to *defect*. This means that, it should not matter what player 1 chooses, player 2 should always choose to defect. This is precisely the Nash equilibrium of the game, and the only one it has. This is precisely what the experiments of [Li and Taplin \(2002\)](#) and [Tversky and Shafir \(1992\)](#) show: although there are variations in the decisions of the players, the majority still choose the optimal decision, which is to defect. Current frameworks, cannot easily accommodate these variations within a mathematical framework, while the quantum-like Bayesian network and the proposed quantum-like influence diagram can.

[Table 5](#) presents the results of both the quantum-like influence diagrams (using the quantum interference computed in the last section) and the classical influence diagram. Both models reflect the general tendency of the decision-makers choosing the optimal strategy, which is in accordance to classical theory. Results also show that, if one wants to explain the violations to the Sure Thing Principle observed in the experiments of [Li and Taplin \(2002\)](#) and [Tversky and Shafir \(1992\)](#) within a maximum expected utility framework, it seems that one cannot adjust directly the quantum interference terms according to the law of maximum entropy and the dynamic similarity heuristic. Although these predictive functions are successful in order to accommodate and predict general probability distributions, they are no longer valid that were observed in the experiments of the literature. This analysis seems to indicate that the quantum interference terms should be found under the definition of a decision problem (where utilities between gambles are incorporated) rather than under the statistical probabilistic space of the experimental problem.

In this sense, we performed a similar analysis as in [Section 5](#), but instead of using the predictive functions proposed in [Moreira and Wichert \(2016a\)](#) and [Wichert and Moreira \(2018\)](#), we analysed how the uncertainty of the decision-maker evolved in the belief space with quantum interference. [Fig. 16](#), shows a density plot of the regions where the decision-maker perceives an expected utility of cooperating to be higher than the expected utility of defecting, $MEU[\text{Cooperate}] > MEU[\text{Defect}]$, in the experiment of [Tversky and Shafir \(1992\)](#).

[Fig. 16](#) shows that one can indeed find regions in the decision-maker's belief state where decision-maker perceives that he will benefit more from a cooperate action, rather than a defect one, $MEU[\text{Cooperate}] > MEU[\text{Defect}]$. This region, however, is small compared to the region where the decision-maker has a higher utility of defecting, $MEU[\text{Defect}] > MEU[\text{Cooperate}]$. In the analysis that we performed for [Tversky and Shafir \(1992\)](#) experiment, we found that the percentage of decision-maker's belief space that would favour a cooperate decision under the quantum-like

influence diagrams would be approximately 13%. On the other hand, the percentage of the belief space that would favour a defect decision would be approximately 87%. These findings are again closely related to the experimental findings of [Tversky and Shafir \(1992\)](#), indicating that most decision-makers prefers to choose the action that leads to the Nash equilibrium, *Defect*, however, sometimes, according the decision-maker prefers to *Cooperate*. This region where the MEU of *Cooperate* is bigger than the MEU of *Defect* can be described by the boundaries of the quantum interferences $\theta_{\text{Def}} \in [0.83\pi, 1.8\pi]$ and $\theta_{\text{Coop}} \in [0\pi, 2\pi]$.

In the next section, we will take a closer look at how the decision-maker's beliefs evolve and change under the quantum-like influence diagrams formalism.

5.4. Evolution of decision-makers change of mind through quantum interference

This section analyses the evolution of decision-maker's beliefs within the framework of the quantum-like influence diagrams. More specifically, we will analyse different levels of decisions under uncertainty ranging from (1) fully rational and optimal decisions (*fully classical*) that follow the axioms of expected utility (connected to rational theories of choice in Economics) ([von Neumann & Morgenstern, 1953](#)), (2) sub-optimal decisions that deviate from the predictions of expected utility theory, but still provide satisfying utilities to the decision-maker (connected to the theories of bounded rationality [Gigerenzer & Goldstein, 1996](#); [Griffiths et al., 2008](#)), to (3) irrational decisions ([Tversky & Shafir, 1992](#)) (*fully quantum*) that reflect the choice of decisions that lead to lower utilities (connected to paradoxical decisions and cognitive bias).

[Fig. 17](#) shows the evolution of the decision-maker's beliefs in the experiment conducted by [Tversky and Shafir \(1992\)](#). In this figure, one can see the following:

- **Fully classical decisions:** the majority of the decision-makers are stable in the regions of the belief space where the MEU of defect is maximised. This notion is in accordance with predictions from expected utility theory and concepts from Game Theory, where in strictly dominant strategies, the decision-maker stays stable in the Nash equilibrium state, in this case, engaging in a defect strategy. In this region, it seems that the decision-maker is not experiencing much uncertainty, and consequently quantum interference effects are minimum.
- **Sub-Optimal decisions:** the lighter regions of the figure indicate decisions where the MEU of defecting is close to the MEU of cooperate, $MEU(\text{Defect}) \approx MEU(\text{Cooperate})$, but still the decision-maker prefers to defect. Quantum interference effects occur and uncertainty is high, however the quantum interference effects are not strong enough to make the decision-maker change his mind and for that reason they continue to choose according to expected utility.
- **Irrational decisions:** correspond to the central, blue regions of the figure. In these regions, uncertainty is maximised and quantum interference effects are significant enough to make the decision-maker change his mind. It is in this region where the decision-maker perceives that $MEU(\text{Cooperate}) > MEU(\text{Defect})$, and consequently is making a decision that deviates from the classical notions of the Expected Utility theory. Notions of game theory actually accept the fact that the decision-maker might not always obey to the formalisms of expected utility theory and be irrational. This might be when players did not understand the rules of the game, or simply because they played randomly. What game theory notions tell us is that the decision-maker will not

Table 5

Maximum expected utility computed using the quantum-like influence diagrams, using the Law of Balance + Max Entropy and the Bayes normalisation + similarity heuristic.

Experiments Literature	Pr(Defect): Condition 3	Classical: MEU (Defect)	Classical MEU (Cooperate)	Law of Balance: MEU (Defect)	Law of Balance: MEU (Cooperate)	Law of Balance: Law Max Entropy	Bayes Norm: MEU (Defect)	Bayes Norm: MEU (Cooperate)	Bayes Norm: Similarity Heuristic
Shafir and Tversky (1992)	0.6300	104.075	9.500	95.2874	17.1414	$\theta_{Def} = \theta_{Coop} = 0$	73.689	35.9225	$\theta_{Def} = \theta_{Coop} = 2.8057$
Li and Taplin (2002) Game 1	0.6000	80.5173	29.985	46.2459	59.7862	$\theta_{Def} = \theta_{Coop} = 0$	72.5042	36.9529	$\theta_{Def} = \theta_{Coop} = 2.9845$
Li and Taplin (2002) Game 2	0.6300	123.769	21.665	89.6398	43.2659	$\theta_{Def} = \theta_{Coop} = 0$	110.778	29.8871	$\theta_{Def} = \theta_{Coop} = 3.0436$
Li and Taplin (2002) Game 3	0.8667	101.585	7.116	88.3079	14.1584	$\theta_{Def} = \theta_{Coop} = 0$	93.2978	11.5116	$\theta_{Def} = \theta_{Coop} = 2.9810$
Li and Taplin (2002) Game 4	0.7000	134.747	29.519	104.619	58.9167	$\theta_{Def} = \theta_{Coop} = 0$	121.129	42.8072	$\theta_{Def} = \theta_{Coop} = 3.0306$
Li and Taplin (2002) Game 5	0.7000	100.262	12.135	73.2732	23.9430	$\theta_{Def} = \theta_{Coop} = 0$	89.6721	16.7685	$\theta_{Def} = \theta_{Coop} = 2.8511$
Li and Taplin (2002) Game 6	0.8000	72.000	8.600	54.2514	17.0800	$\theta_{Def} = \theta_{Coop} = 0$	64.5224	12.1726	$\theta_{Def} = \theta_{Coop} = 2.9350$
Li and Taplin (2002) Game 7	0.7667	72.000	8.600	55.0305	16.7077	$\theta_{Def} = \theta_{Coop} = 0$	64.4312	12.2162	$\theta_{Def} = \theta_{Coop} = 2.7365$

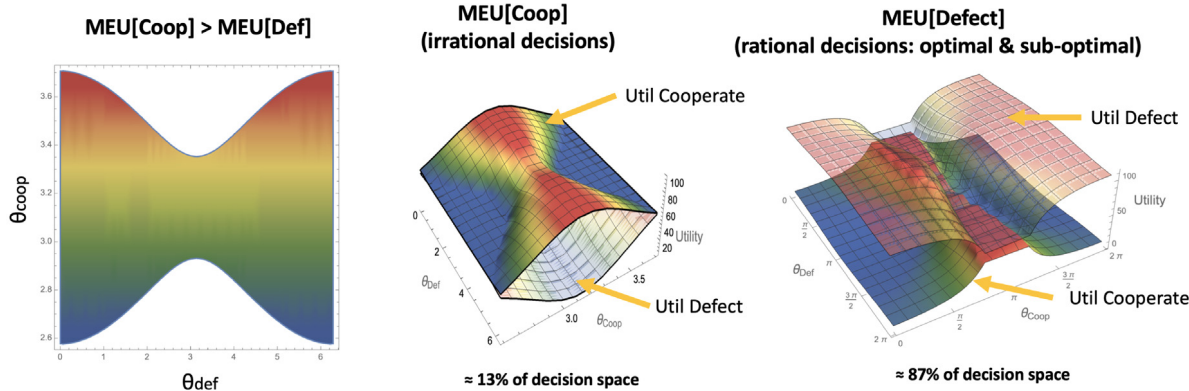


Fig. 16. Analysis of the decision-maker's belief space with different quantum interference effects. One can see that there are regions in the belief space where the decision-maker perceives that he benefits from a cooperate action over a defect one.

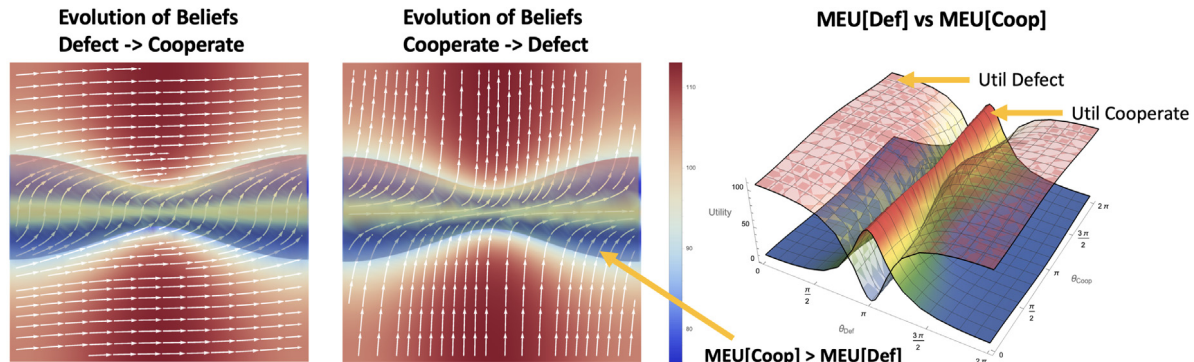


Fig. 17. Evolution of the decision-maker's beliefs from a defect decision towards a cooperate one in Tversky and Shafir (1992) experiment using the influence diagrams together with Bayes normalisation. The utilities that the decision-maker can obtain within this framework are also depicted in the diagram in the right. This diagram shows that there are some regions, where the decision-maker perceives a higher utility by choosing to Cooperate, rather than to Defect.

stay stable in these irrational states. That is exactly what Fig. 17 shows. Although some decision-makers perceive that to Cooperate is the best action, they do not stay stable in that state.

The same analysis was done, but this time, using the law of balance as a normalisation procedure (Fig. 18). As one can see from the utility diagram, the wave that promotes the Defect strategy completely dominates the wave that promotes cooperation. Under this setting, the decision-maker will always perceive that $MEU[\text{Defect}] > MEU[\text{Cooperate}]$, independently of the uncertainty he is experiencing and for this reason, the decision-maker will always act according to what is predicted according to classical theory.

We extended the analysis for the remaining experiments performed by Li and Taplin (2002) using the Bayes normalisation. The results can be found in Fig. 19 and similar findings to the ones highlighted in Tversky and Shafir (1992) have been found: the majority of the decision-maker's prefer to stay in the Nash

equilibrium by keeping the Defect strategy. However, there are some set of participants that experience high levels of uncertainty, and consequently are strongly affected by quantum interference effects, which makes them perceive $MEU[\text{Cooperate}] > MEU[\text{Defect}]$.

6. Connection to Hebb's assembly theory

It is important to note that this research is not concerned with modelling the brain with quantum theory, nor is directly concerned with the idea that brain is a quantum computer (Busemeyer & Bruza, 2012). Instead, our model assumes that quantum wave functions are present in the macroscopic world, like it has been confirmed in a variety of scientific studies (Amico et al., 2008; Ghosh et al., 2003; Vedral, 2011). However, if such architecture had to be implemented, one can assume that the proposed quantum-like influence diagram is a theoretical assembly model that explains how stimuli represented by assemblies of neurons can be propagated during the decision process. In this model, we

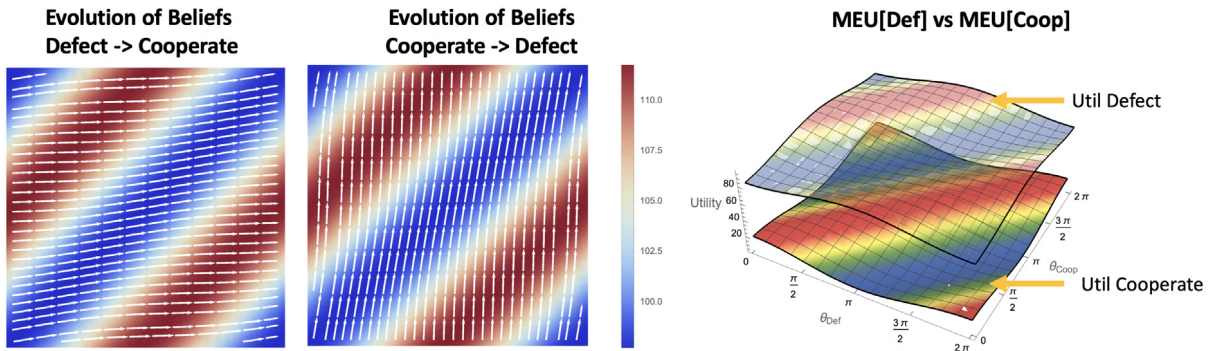


Fig. 18. Evolution of the decision-maker's beliefs from a defect decision towards a cooperate one in Tversky and Shafir (1992) experiment using the influence diagrams together with the law of balance. The utilities that the decision-maker can obtain within this framework are also depicted in the diagram in the right. This diagram shows that there the decision-maker never prefers to Cooperate within the Law of Balance formalism, since one of the waves fully dominates the other.

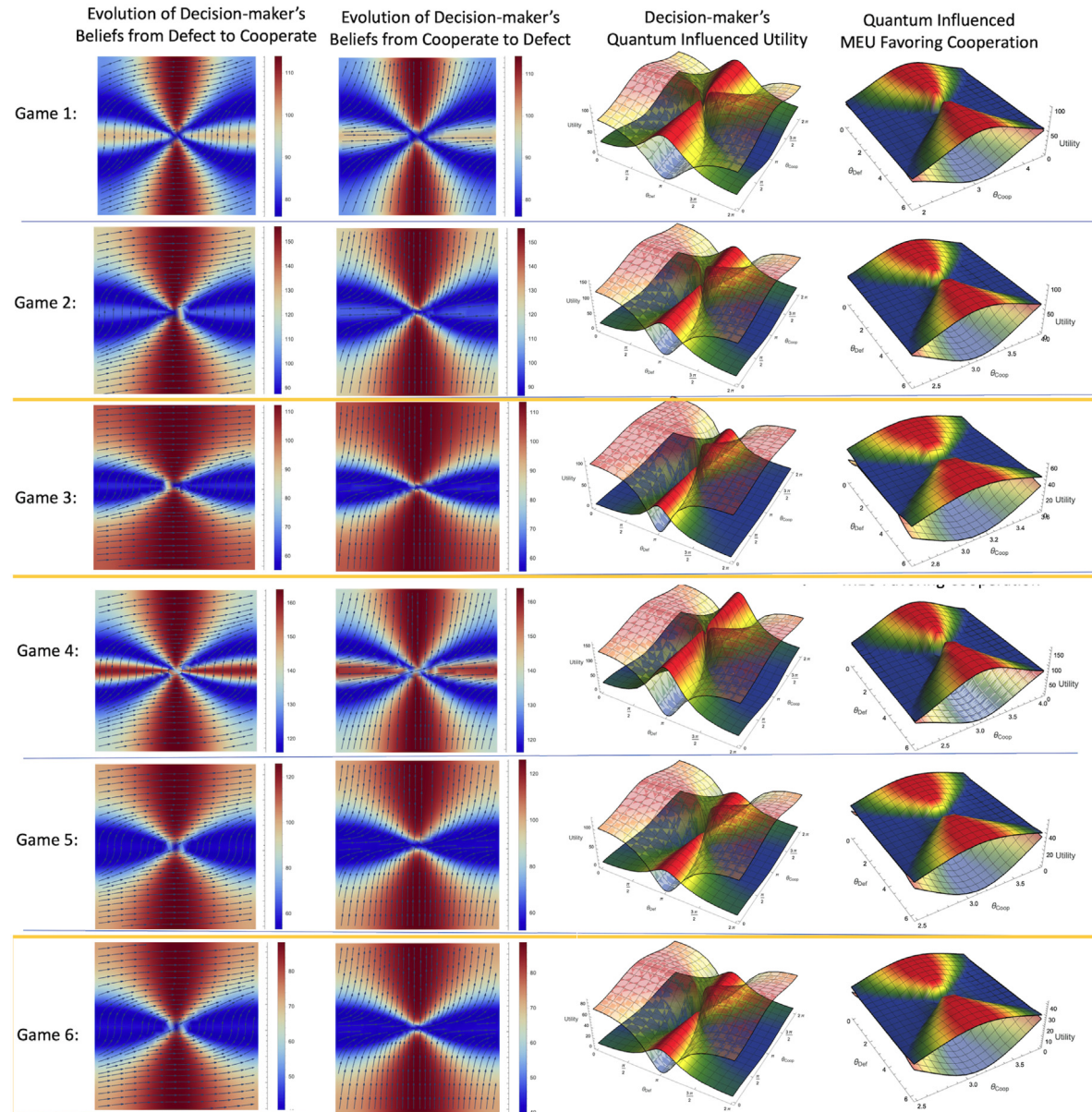


Fig. 19. Evolution of the decision-maker's belief state for the experiments conducted by Li and Taplin (2002). One can notice that the majority of the decision-makers act according to expected utility theory, however one can identify some regions where the decision-maker perceives that the $MEU(\text{Cooperate}) > MEU(\text{Defect})$. The regions that are highlighted correspond to experiments where violations of the Sure Thing Principle were not present. One can notice that quantum interference effects are minimum and beliefs with $MEU(\text{Defect}) > MEU(\text{Cooperate})$ almost overtake the entire space.

assume that the cell of assemblies of a Neural Network act in the same way as graph, where each cell assembly of a neuron corresponds to a node, and the connection between the assemblies corresponds to the links that represent conditional probabilities. If a cell neither fires nor has a negative influence firing through inhibitory connections, it is assumed that the cell is in a kind of superposition. Consequently, the law of total probability attenuated by an interference term is applied. This notion is inspired by the neural assembly theory introduced by Donald Hebb (Hebb, 1949). He proposed a connection between the structures found in the nervous system and those involved in high-level cognition such as diagnostic problem solving. An assembly of neurons acts as a closed system, and can therefore represent a complex object. Activation of some neurons of the assembly leads to the activation of the entire assembly, so that manipulations on the representation of a complex object are performed (Hebb, 1958). Our model is a theoretical assembly model that explains how stimuli represented by assemblies can be propagated during the decision making process. In our model an assembly may be in four states: (1) not activated since it is not working, (2) positively activated, (3) negative activated or (4) in a superposition state that is neither, positively activated or negatively activated. The connections between the assemblies correspond to the conditional probability values and are represented under the framework of probabilistic graphical models.

7. Conclusions

In this paper, we put together a full decision framework based on quantum probability theory in order to describe the probabilistic nature of the human decision-making process with a focus on modelling paradoxical human decisions reported in several works of the literature. This work is motivated by the fact that, when dealing with preferences under uncertainty, it seems that models based on normative theories of rational choice tend to tell how individuals *must* choose, instead of telling how individuals *actually* choose (Machina, 2009). Our main thesis is that models that could take into account sub-optimal and paradoxical human decisions could greatly improve decision support systems.

We propose a new comprehensive framework on how to describe the probabilistic nature of the human decision-making process with a focus on modelling paradoxical, sub-optimal and irrational human decisions by extending the quantum-like Bayesian network formalism to incorporate the notion of maximum expected utility through the notion of quantum-like influence diagrams. In this model, instead of proposing an alternative representation of the expected utility theory, we retain expected utility as it is commonly understood, but we take advantage of the quantum interference terms produced in the quantum-like Bayesian Network to influence the probabilities used to compute the expected utility of some action.

Experimental results showed that the proposed model is able to (1) accommodate the different paradoxical findings reported in different experiments of the literature, through the quantum-like probabilistic inferences of the quantum-like Bayesian network, (2) augment the decision-making system by capturing human decisions that are considered paradoxical, and therefore classified as irrational, by using quantum interference to quantify the decision-maker's uncertainty; This quantum interference can provide us new insights from the decision-maker's belief space and help understand in which regions in this space, the decision-maker perceives that choosing the irrational decision would give him a higher maximum expected utility, and (3) be able to study the evolution of the decision-maker's belief within his belief space, through quantum interference.

We believe that this model can be a foundation for new decision support systems that are able to quantify human uncertainty and ambiguity under a quantum-like mathematical framework. The initial results are very promising, and they suggest the potential of new insights decision science with direct implications in decision support systems that deal with human data, such as economics, finance, psychology, etc. A promising path includes models for social-ecological systems, such as participatory Bayesian networks that explore ambiguity among stakeholders (Sallou, Barnaud, Vialatte, & Monteil, 2017), that try to promote decision models for more sustainable activities.

Declaration of competing interest

The authors declare that they have no known competing financial interests or personal relationships that could have appeared to influence the work reported in this paper.

Acknowledgements

Dr. Andreas Wichert was supported by funds through Fundação para a Ciência e Tecnologia (FCT), Portugal with reference UID/CEC/50021/2019. The funders had no role in study design, data collection and analysis, decision to publish, or preparation of the manuscript.

Appendix A. Some notes on notation and representation

The notation adopted in quantum theory is the Dirac notation, also known as the “bra-ket” notation. Instead of writing states using column vectors, in quantum theory column vectors are written in a linear and compact way. For instance, a k -dimensional column vector A

$$A = \begin{pmatrix} \alpha_0 \\ \alpha_1 \\ \vdots \\ \alpha_{k-1} \end{pmatrix}$$

can be written in terms of *ket* notation as $|A\rangle$, in the following way

$$|A\rangle = \alpha_0|0\rangle + \alpha_1|1\rangle + \cdots + \alpha_{k-1}|k-1\rangle,$$

where $|0\rangle, |1\rangle \dots$ are basis vectors with the following representation

$$|0\rangle = \begin{pmatrix} 1 \\ 0 \\ \vdots \\ 0 \end{pmatrix}, |1\rangle = \begin{pmatrix} 0 \\ 1 \\ \vdots \\ 0 \end{pmatrix}, \dots, |k-1\rangle = \begin{pmatrix} 0 \\ 0 \\ \vdots \\ 1 \end{pmatrix}$$

The *bra* notation, of the same vector, $\langle A|$, corresponds to the conjugate transpose (represented in this article by the symbol \dagger) of the *ket* representation:

$$\langle A| = \langle A|^{\dagger}$$

This means that the inner product of vector A can be expressed as

$$\langle A|A \rangle = (\alpha_0^* \quad \alpha_1^* \quad \dots \quad \alpha_{k-1}^*) \begin{pmatrix} \alpha_0 \\ \alpha_1 \\ \vdots \\ \alpha_{k-1} \end{pmatrix} = |\alpha_0|^2 + |\alpha_1|^2 + \cdots + |\alpha_{k-1}|^2.$$

Algorithm 1 Quantum-Like Bayesian Network**Require:** \mathbb{F} , factor structure

ObservedVars, list of observed variables,

QueryVar, identifier of the variable to be queried,

Ensure: Factor Q , corresponding to the quantum inferences,
Factor C , corresponding to the classical inferences

- 1: /* A factor is a structure containing three lists:
 var , corresponds to an identifier of a random variable. It also contains the list of the parent vars.
 $card$, corresponds to the cardinality of each random variable in var.
 val , corresponds to the respective conditional probability table. */
- 2: $Q \leftarrow \text{struct}('var', \text{QueryVar}, 'card', 2, \text{val}, \{\})$; // initialise output factor structure for quantum network
- 3: $C \leftarrow \text{struct}(var, \text{QueryVar}, 'card', 2, \text{val}, \{\})$; // initialise output factor structure for classical network
- 4: // Observe evidence: set to 0 all factors in \mathbb{F} that do not correspond to the evidence variables
- 5: $\mathbb{F} \leftarrow \text{ObserveEvidence}(\mathbb{F}, \text{ObservedVars});$
- 6: // Compute the Full Joint Probability Distribution of the Network:
- 7:
- 8: $Joint \leftarrow \text{ComputeFullJointDistribution}(\mathbb{F});$
- 9: // Marginalise the full joint probability distribution. Select the positive and negative assignments of QueryVar:
- 10: $[\text{PositiveProb}, \text{NegativeProb}] \leftarrow \text{FactorMarginalization}(Joint, \text{QueryVar});$
- 11: // Compute classical probability factor by applying Eq. (2)
- 12: $C.\text{val} \leftarrow \text{ComputeClassicalProb}(\text{PositiveProb}, \text{NegativeProb});$
- 13: // Compute quantum probability factor according to Algorithm 2
- 14: $Q.\text{val} \leftarrow \text{ComputeQuantumProb}(\text{PositiveProb}, \text{NegativeProb});$
- 15: **return** $[Q, C];$

In the same way, the outer product of vector A , which is also known as the *quantum Projection operator*, can be expressed as

$$\begin{aligned} |A\rangle\langle A| &= \begin{pmatrix} \alpha_0 \\ \alpha_1 \\ \vdots \\ \alpha_{k-1} \end{pmatrix} (\alpha_0^* & \alpha_1^* & \dots & \alpha_{k-1}^*) \\ &= \begin{pmatrix} |\alpha_0|^2 & \alpha_0\alpha_1^* & \dots & \alpha_0\alpha_{k-1}^* \\ \alpha_1\alpha_0^* & |\alpha_1|^2 & \dots & \alpha_1\alpha_{k-1}^* \\ \vdots & \vdots & \ddots & \vdots \\ \alpha_{k-1}\alpha_0^* & \alpha_{k-1}\alpha_1^* & \dots & |\alpha_{k-1}|^2 \end{pmatrix}, \\ &\text{where } |\alpha_0|^2 + |\alpha_1|^2 + \dots + |\alpha_{k-1}|^2 = 1 \end{aligned}$$

The main advantage of using Dirac's notation is that it enables the explicit labelling of the basis vectors, which plays an important role in quantum theory and the quantum-like model that we will present in the next section.

Appendix B. Notes on the application of quantum-like Bayesian networks**B.1. Quantum states**

Consider the example of Fig. 2. For simplicity, let us assume that the random variables are all binary with basis vectors $|0\rangle$

and $|1\rangle$. One can represent the child state $|\psi_{X2}\rangle$ as an *ensemble* of two states: one representing the probability distributions if that state requires information about the state $|\psi_{X1=0}\rangle$, which is represented by the notation $|\psi_{X2|X1=0}\rangle$; and another representing the probability distributions if that state requires information about the state $|\psi_{X1=1}\rangle$, which is represented by the notation $|\psi_{X2|X1=1}\rangle$.

$$\begin{aligned} |\psi_{X2|X1=0}\rangle &= \beta_{00}|0\rangle + \beta_{01}|1\rangle \text{ where } |\beta_{00}|^2 + |\beta_{01}|^2 = 1 \\ |\psi_{X2|X1=1}\rangle &= \beta_{10}|0\rangle + \beta_{11}|1\rangle \text{ where } |\beta_{10}|^2 + |\beta_{11}|^2 = 1 \end{aligned} \quad (\text{B.1})$$

The child quantum state $|\psi_{X2}\rangle$ is simply the matrix representation of the states $|\psi_{X2|X1=0}\rangle$ and $|\psi_{X2|X1=1}\rangle$,

$$|\psi_{X2}\rangle = \begin{pmatrix} \beta_{00} & \beta_{10} \\ \beta_{01} & \beta_{11} \end{pmatrix} \quad (\text{B.2})$$

In Fig. 2, state $|\psi_{X3}\rangle$ is given by an analogous ensemble:

$$\begin{aligned} |\psi_{X2|X1=0}\rangle &= \beta_{00}|0\rangle + \beta_{01}|1\rangle \text{ where } |\beta_{00}|^2 + |\beta_{01}|^2 = 1 \\ |\psi_{X2|X1=1}\rangle &= \beta_{10}|0\rangle + \beta_{11}|1\rangle \text{ where } |\beta_{10}|^2 + |\beta_{11}|^2 = 1 \end{aligned} \quad (\text{B.3})$$

Algorithm 2 ComputeQuantumProbability

Require: *PositiveProb*, vector of marginal probabilities when *QueryVar* occurs,
NegativeProb, vector of marginal probabilities when *QueryVar* does not occur,
Ensure: List *Q* with probabilistic inference using quantum theory

```

1: interference_pos  $\leftarrow 0$ ;
2: length_assign  $\leftarrow \text{length}(\text{PositiveProb})$ ;

3: // For all probability assignments,
4: for i = 1; i  $\leq \text{length\_assign} - 1$ ; i = i + 1 do
5:   for j = i + 1; j  $\leq \text{length\_assign}$ ; j = j + 1 do
6:     // Compute the quantum interference parameter  $\theta$  according to a given heuristic function
7:     heurs  $\leftarrow \text{SimilarityHeuristic}(\text{PosAssign}, \text{NegAssign})$ 

8:     // Apply quantum interference formula:
9:

$$\sum_{i=1}^{|Y|-1} \sum_{j=i+1}^{|Y|} \left| \prod_k^N \psi(X_k | \text{Parents}(X_k), e, y = i) \right| \cdot$$


$$\cdot \left| \prod_k^N \psi(X_k | \text{Parents}(X_k), e, y = j) \right| \cdot \cos(\theta_i - \theta_j);$$


10:    // Compute the interference term related to the positive assignments
11:    interference_pos  $\leftarrow \text{interference_pos} + 2\text{PosAssign}[i]\text{PosAssign}[j] \text{ heurs}$ 
12:
13:    // Compute the interference term related to the negative assignments (for normalisation)
14:    interference_neg  $\leftarrow \text{interference_neg} + 2\text{NegAssign}[i]\text{NegAssign}[j] \text{ heurs}$ 

15:  end for
16: end for
17: // Compute quantum-like probabilities: classicalProb + interference.
18:  $\alpha = (\text{sum}(\text{PosAssign}) + \text{sum}(\text{NegAssign}))^{-1}$ 
19: classicalProb  $\leftarrow [\alpha \text{ PosAssign}, \alpha \text{ NegAssign}]$ ;
20: probPos  $\leftarrow \text{classicalProb}[1] + \text{interference\_pos}$ ;
21: probNeg  $\leftarrow \text{classicalProb}[2] + \text{interference\_neg}$ ;

22: // Normalise the results in order to obtain a probability value
23:  $\gamma \leftarrow (\text{probPos} + \text{probNeg})^{-1}$ 
24: Q  $\leftarrow [\gamma \text{ probPos}, \gamma \text{ probNeg}]$ 

25: return Q;

```

And state $|\psi_{X_4}\rangle$ is given by an ensemble containing $|\psi_{X_2}\rangle$ and $|\psi_{X_3}\rangle$.

$$\begin{aligned}
|\psi_{X_4}|_{X_2=0,X_3=0}\rangle &= \gamma_{000}|0\rangle + \gamma_{001}|1\rangle \quad \text{where } |\gamma_{000}|^2 + |\gamma_{001}|^2 = 1 \\
|\psi_{X_4}|_{X_2=0,X_3=1}\rangle &= \gamma_{010}|0\rangle + \gamma_{011}|1\rangle \quad \text{where } |\gamma_{010}|^2 + |\gamma_{011}|^2 = 1 \\
|\psi_{X_4}|_{X_2=1,X_3=0}\rangle &= \gamma_{100}|0\rangle + \gamma_{101}|1\rangle \quad \text{where } |\gamma_{100}|^2 + |\gamma_{101}|^2 = 1 \\
|\psi_{X_4}|_{X_2=1,X_3=1}\rangle &= \gamma_{110}|0\rangle + \gamma_{111}|1\rangle \quad \text{where } |\gamma_{110}|^2 + |\gamma_{111}|^2 = 1,
\end{aligned} \tag{B.4}$$

which translates into state:

$$|\psi_{X_4}\rangle = \begin{pmatrix} \gamma_{000} & \gamma_{010} & \gamma_{100} & \gamma_{110} \\ \gamma_{001} & \gamma_{011} & \gamma_{101} & \gamma_{111} \end{pmatrix} \tag{B.5}$$

B.2. Density operator and partial trace

Consider again the example in Fig. 2. If we would like to examine more closely the subsystem of the quantum states shared by just ψ_{X_1} and ψ_{X_3} , we need to take the trace over ψ_{X_2} and ψ_{X_4} . This operation will sum out the variables in X_2 and X_4 , reducing

the size of the 16×16 matrix to a subsystem of size 4×4 given in Box I.

Considering the example in Fig. 2, if one wants to compute the probability of $\Pr(X_1 = 1)$, then, one would need to first compute the partial trace over the variables X_2 and X_4 and define the operator M as

$$\Pr(X_1 = 1, X_3 = 0) = \langle M_{X_1=1, X_3=0} | \text{Tr}_{X_2, X_4} [\rho_G(X_1, X_2, X_3, X_4)] | M_{X_1=1, X_3=0} \rangle$$

$$\text{where } |M_{X_1=1, X_3=0}\rangle = \begin{pmatrix} 0 & & & \\ 0 & & & \\ 1 & & & \\ 0 & & & \end{pmatrix}_{\substack{|X_1=0, X_3=0| \\ |X_1=0, X_3=1| \\ |X_1=1, X_3=0| \\ |X_1=1, X_3=1|}}$$

Appendix C. Example of application of quantum-like influence diagrams to the Prisoner's Dilemma game

Starting with the experiment from Tversky and Shafir (1992) which is represented in Fig. 11, one can define the density operator ρ_G in order to express the networks (5).

$$\rho_{\mathcal{G}(X_1, X_3)} = Tr_{X_2, X_4} [\rho_{\mathcal{G}(X_1, X_2, X_3, X_4)}] = \\ = \begin{pmatrix} a_{00,00} + a_{01,01} + a_{04,04} + a_{05,05} & a_{00,02} + a_{01,03} + a_{04,06} + a_{05,07} & a_{00,08} + a_{01,09} + a_{04,12} + a_{05,13} & a_{00,10} + a_{01,11} + a_{04,14} + a_{05,15} \\ a_{02,00} + a_{03,01} + a_{06,04} + a_{07,05} & a_{02,02} + a_{03,03} + a_{06,06} + a_{07,07} & a_{02,08} + a_{03,09} + a_{06,12} + a_{07,13} & a_{02,10} + a_{03,11} + a_{06,14} + a_{07,15} \\ a_{08,00} + a_{09,01} + a_{12,04} + a_{13,05} & a_{08,02} + a_{09,03} + a_{12,06} + a_{13,07} & a_{08,08} + a_{09,09} + a_{12,12} + a_{13,13} & a_{08,10} + a_{09,11} + a_{12,14} + a_{13,15} \\ a_{10,00} + a_{11,01} + a_{14,04} + a_{15,05} & a_{10,02} + a_{11,03} + a_{14,06} + a_{15,07} & a_{10,08} + a_{11,09} + a_{14,12} + a_{15,13} & a_{10,10} + a_{11,11} + a_{14,14} + a_{15,15} \end{pmatrix} \quad (B.6)$$

Box I.

Algorithm 3 SimilarityHeuristic

Require: *PositiveProb*, vector of marginal probabilities when *QueryVar* occurs,
NegativeProb, vector of marginal probabilities when *QueryVar* does not occur,
Ensure: *interf*, Quantum Interference term

```

1: // Compute Euclidean distances between vectors
2: normc ← norm(PosProb – NegProb, 2);
3: norma ← norm(PosProb, 2);
4: normb ← norm(PosNeg, 2);

5: // Compute angles between vectors using the law of cosines
6:  $\theta_a \leftarrow ACos(\frac{\text{norm}_b^2 - \text{norm}_a^2 + \text{norm}_c^2}{2 * \text{norm}_c * \text{norm}_b})$ ;
7:  $\theta_b \leftarrow ACos(\frac{\text{norm}_a^2 - \text{norm}_b^2 + \text{norm}_c^2}{2 * \text{norm}_c * \text{norm}_a})$ 
8:  $\theta_c \leftarrow ACos(\frac{\text{norm}_a^2 + \text{norm}_b^2 - \text{norm}_c^2}{2 * \text{norm}_a * \text{norm}_b})$ ;

9: // Compute de similarity measure  $\phi$ 
10:  $\phi \leftarrow \frac{\theta_c}{\theta_a} - \frac{\theta_b}{\theta_a}$ ;
```

11: // Apply heuristic using the thresholds according ([Moreira & Wichert, 2016a](#))
12: *interf* ← 0;

```

13: if  $\phi < -2$  then
14:   interf ← 1.5408;
15: end if
16: if  $\phi >= -2$  &&  $\phi <= 0$  then
17:   interf ← 1.5178
18: end if
19: if  $\phi >= 0.15$  then
20:   interf ←  $\pi$ 
21: end if
22: return Cos(interf);
```

The system's superposition state is given by

$$|S_G\rangle = \begin{pmatrix} \psi(P1_d)\psi(P2_d|P1_d)e^{i\theta_1} \\ \psi(P1_d)\psi(P2_c|P1_d)e^{i\theta_2} \\ \psi(P1_c)\psi(P2_d|P1_c)e^{i\theta_3} \\ \psi(P1_c)\psi(P2_c|P1_c)e^{i\theta_4} \end{pmatrix} = \begin{pmatrix} 0.696419e^{i\theta_1} \\ 0.122474e^{i\theta_2} \\ 0.648074e^{i\theta_3} \\ 0.282843e^{i\theta_4} \end{pmatrix},$$

$$\text{where } \sum_i \sum_j |\psi(P1_i)\psi(P2_j|P1_i)|^2 = 1,$$

which results in the density operator, $\rho_{\mathcal{G}}$, given in [Box II](#)

From the density operator, $\rho_{\mathcal{G}}$, one can compute the *classical full joint probability distribution* of the network if we extract the elements of the *main diagonal*. In other words,

$$Joint = Diag(\rho_{\mathcal{G}(P1, P2)}) = (0.485 \ 0.015 \ 0.42 \ 0.08).$$

The quantum interference terms are located in the off-diagonal positions of $\rho_{\mathcal{G}(P1, P2)}$. It is precisely through these off-diagonal elements that, during the inference process, one is

able to obtain quantum interference effects, and consequently, deviations from classical probabilistic inferences.

From the density operator $\rho_{\mathcal{G}(P1, P2)}$, one can compute the probabilistic inferences of each of the decision-maker's actions by performing the Partial Trace operation over the random variable *BeliefPlayer1Action* and by selecting the entries of the resulting distribution that match the decision-makers decision, $|Def\rangle$. This results in the probabilities,

$$\begin{aligned}
Pr(P2_d) &= \langle Def | Tr_{P1}(\rho_{\mathcal{G}(P1, P2)}) | Def \rangle \\
&= 0.905 + 0.902663 \cos(\theta_{def} - \theta_{coop}) \\
\text{where, } |Def\rangle &= \begin{pmatrix} 1 \\ 0 \\ 1 \\ 0 \end{pmatrix}
\end{aligned} \quad (C.2)$$

In the same way, we can compute the probability of the decision-maker cooperating by simply choosing another operator that will select only the cooperate decisions out of the density

$$\rho_{G(P1,P2)} = |S_G\rangle\langle S_G| = \begin{pmatrix} 0.485 & 0.0852936e^{i(\theta_1-\theta_2)} & 0.451331e^{i(\theta_1-\theta_3)} & 0.196977e^{i(\theta_1-\theta_4)} \\ 0.0852936e^{-i(\theta_1-\theta_2)} & 0.015 & 0.0793725e^{i(\theta_2-\theta_3)} & 0.034641e^{i(\theta_2-\theta_4)} \\ 0.451331e^{-i(\theta_1-\theta_3)} & 0.0793725e^{-i(\theta_2-\theta_3)} & 0.42 & 0.183303e^{i(\theta_3-\theta_4)} \\ 0.196977e^{-i(\theta_1-\theta_4)} & 0.034641e^{-i(\theta_2-\theta_4)} & 0.183303e^{-i(\theta_3-\theta_4)} & 0.08 \end{pmatrix} \quad (C.1)$$

Box II.

matrix,

$$\Pr(P2_c) = \langle \text{Coop} | Tr_{P1}(\rho_{G(P1,P2)}) | \text{Coop} \rangle \\ = 0.095 + 0.069282 \cos(\theta_{\text{def}} - \theta_{\text{coop}}) \\ \text{where, } |\text{Coop}\rangle = \begin{pmatrix} 0 \\ 1 \\ 0 \\ 1 \end{pmatrix} \quad (C.3)$$

Appendix D. QuLBiT: Quantum-like Bayesian inference technologies

The quantum-like Bayesian Network proposed in Moreira and Wichert (2016a) is built in a similar way as a classical network, with the difference that it uses complex amplitudes to specify the conditional probability tables, instead of real probability values. As a consequence, the quantum-like Bayesian Network will give rise to interference effects, which can act destructively or constructively if the interferences are negative or positive, respectively.

Algorithm 1 describes the main steps to compute quantum-like inferences. Basically, a probabilistic inference consists of two major steps: the computation of the full joint probability distribution of the network and the computation of the marginal probability distribution with respect to the variable being queried.

Appendix E. The similarity heuristic for interference effects

See Algorithms 1–3.

References

- Aaronson, S. (2013). *Quantum computing since democritus*. Cambridge University Press.
- Aerts, D., Broekaert, J., & Smets, S. (2004). A quantum structure description of the liar paradox. *International Journal of Theoretical Physics*, 38, 3231–3239.
- Aerts, D., Gerente, S., Moreira, C., & Sozzo, S. (2017). Testing ambiguity and Machina preferences within a quantum-theoretic framework for decision-making. *Journal of Mathematical Economics*.
- Allais, M. (1953). Le comportement de l'homme rationnel devant le risque: Critique des postulats et axiomes de l'école américaine. *Econometrica*, 21, 503–546.
- Amico, L., Fazio, R., Osterloh, A., & Vedral, V. (2008). Entanglement in many-body systems. *Reviews of Modern Physics*, 80, 517–576.
- Baeza-Yates, R., & Ribeiro-Neto, B. (2010). *Modern information retrieval: Concepts and technology behind search*. Pearson Education.
- Beck, J. M., Ma, W. J., Pitkow, X., Latham, P. E., & Pouget, A. (2012). More varieties of Bayesian theories, but no enlightenment. *Behaviour and Brain Sciences*, 35, 30–39.
- Birnbaum, M. (2008). New paradoxes of risky decision making. *Psychological Review*, 115, 463–501.
- Boole, G. (1847). *The mathematical analysis of logic*. Cambridge University Press.
- Bowers, J., & Davis, C. (2011). More varieties of Bayesian theories, but no enlightenment. *Behaviour and Brain Sciences*, 34, 193–194.
- Busemeyer, J., & Bruza, P. (2012). *Quantum model of cognition and decision*. Cambridge University Press.
- Busemeyer, J., Wang, Z., & Townsend, J. (2006). Quantum dynamics of human decision making. *Journal of Mathematical Psychology*, 50, 220–241.
- Crosson, R. (1999). The disjunction effect and reason-based choice in games. *Organizational and Human Decision Processes*, 80, 118–133.
- Ellsberg, D. (1961). Risk, ambiguity and the savage axioms. *Quarterly Economics*, 75, 643–669.
- Ghosh, S., Rosenbaum, T. F., Aepli, G., & Coppersmith, S. N. (2003). Entangled quantum state of magnetic dipoles. *Nature*, 425, 48–51.
- Gigerenzer, G., & Goldstein, D. G. (1996). Reasoning the fast and frugal way: Models of bounded rationality. *Psychological Review*, 103, 650–669.
- Griffiths, T., Kemp, C., & Tenenbaum, J. (2008). Bayesian models of inductive learning. In *Proceedings of the annual conference of the cognitive science society*.
- Grossberg, S. (1988). Nonlinear neural networks: Principles, mechanisms, and architectures. *Neural Networks*, 1, 17–61.
- Hebb, D. (1949). *The organization of behavior*. New York: John Wiley.
- Hebb, D. (1958). *Textbook of psychology*. Philadelphia London Toronto: Sanders.
- Hirvensalo, M. (2003). *Quantum computing* (2nd ed.). Springer.
- Hristova, E., & Grinberg, M. (2008). Disjunction effect in prisoner's dilemma: Evidences from an eye-tracking study. In *Proceedings of the 30th annual conference of the cognitive science society*.
- Kahneman, D., Slovic, P., & Tversky, A. (1982). *Judgment under uncertainty: Heuristics and biases*. Cambridge University Press.
- Kahneman, D., & Tversky, A. (1979). Prospect theory – an analysis of decision under risk. *Econometrica*, 47, 263–292.
- Kass, R., & Wasserman, L. (1995). A reference Bayesian test for nested hypotheses and its relationship to the Schwarz criterion. *Journal of the American Statistical Association*, 90, 928–934.
- Koller, D., & Friedman, N. (2009). *Probabilistic graphical models: Principles and techniques*. The MIT Press.
- Lander, D., & Shenoy, P. (2001). *Modeling and valuing real options-using influence diagrams: Technical report*, School of Business, Babson College.
- Leifer, M., & Poulin, D. (2008). Quantum graphical models and belief propagation. *Annals of Physics Journal*, 323, 1899–1946, eprint arxiv-ph/0708.1337 [quant-ph].
- Levine, D. (2009). Brain pathways for cognitive-emotional decision making in the human animal. *Neural Networks*, 22, 286–293.
- Li, S., & Taplin, J. (2002). Examining whether there is a disjunction effect in prisoner's dilemma game. *Chinese Journal of Psychology*, 44, 25–46.
- Lisboa, P., & Taktak, A. (2006). The use of artificial neural networks in decision support in cancer: A systematic review. *Neural Networks*, 19, 408–415.
- Machina, M. (2009). Risk, ambiguity, and the rank-dependence axioms. *Journal of Economic Review*, 99, 385–392.
- Mazurowska, M. A., Habasa, P. A., Zuradaa, J. M., Lob, J. Y., Bakerb, J. A., & Tourassi, G. D. (2008). Training neural network classifiers for medical decision making: The effects of imbalanced datasets on classification performance. *Neural Networks*, 21, 427–436.
- McMahon, D. (2007). *Quantum computing explained*. Wiley-IEEE Computer Society.
- Moreira, C., Fell, L., Dehdashti, S., Bruza, P., & Wichert, A. (2020). Towards a quantum-like cognitive architecture for decision-making. *Behavioral and Brain Sciences*, 43, e17. <http://dx.doi.org/10.1017/S0140525X19001687>.
- Moreira, C., Hammes, M., Kurdoglu, R. S., & Bruza, P. (2020). QuLBiT: Quantum-like Bayesian inference technologies for cognition and decision. In *Proceedings of the 42nd annual meeting of the cognitive science society*.
- Moreira, C., Haven, E., Sozzo, S., & Wichert, A. (2018). Process mining with real world financial loan applications: Improving inference on incomplete event logs. *PLoS One*, 13, Article e0207806.
- Moreira, C., & Wichert, A. (2014). Interference effects in quantum belief networks. *Applied Soft Computing*, 25, 64–85.
- Moreira, C., & Wichert, A. (2016a). Quantum-like Bayesian networks for modeling decision making. *Frontiers in Psychology: Cognition*, 7(11).
- Moreira, C., & Wichert, A. (2016b). Quantum probabilistic models revisited: The case of disjunction effects in cognition. *Frontiers in Physics: Interdisciplinary Physics*, 4, 1–26.
- Moreira, C., & Wichert, A. (2017). Exploring the relations between quantum-like Bayesian networks and decision-making tasks with regard to face stimuli. *Journal of Mathematical Psychology*, 78, 86–95.
- Moreira, C., & Wichert, A. (2018). Are quantum-like Bayesian networks more powerful than classical Bayesian networks? *Journal of Mathematical Psychology*, 28, 73–83.
- Mortera, J., Vicard, P., & Vergari, C. (2013). Object-oriented Bayesian networks for a decision support system for antitrust enforcement. *The Annals of Applied Statistics*, 7, 714–738.
- Mura, P. L. (2009). Projective expected utility. *Journal of Mathematical Psychology*, 53, 408–414.

- von Neumann, J. (1996). *Mathematical foundations of quantum mechanics*. Princeton University Press.
- von Neumann, J., & Morgenstern, O. (1953). *Theory of games and economic behavior*. Princeton University Press.
- Owens, D. K., Shachter, R. D., & Robert F. Nease, J. (1997). Representation and analysis of medical decision problems with influence diagrams. *Medical Decision Making*, 17(3), 241–262.
- Pearl, J. (1988). *Probabilistic reasoning in intelligent systems: Networks of plausible inference*. Morgan Kaufmann Publishers.
- Peters, O. (2019). The ergodicity problem in economics. *Nature Physics*, 15, 1216–1221.
- Pothos, E., & Busemeyer, J. (2009). A quantum probability explanation for violations of rational decision theory. *Proceedings of the Royal Society B*, 276, 2171–2178.
- Russel, S., & Norvig, P. (2010). *Artificial intelligence: A modern approach* (3rd ed.). Pearson Education.
- Salliou, N., Barnaud, C., Vialatte, A., & Monteil, C. (2017). A participatory Bayesian Belief Network approach to explore ambiguity among stakeholders about socio-ecological systems. *Environmental Modelling & Software*, 96, 199–209.
- Savage, L. (1954). *The foundations of statistics*. John Wiley.
- Schwarteneck, P., FitzGerald, T., Mathys, C., Dolan, R., Wurst, F., Kronbichler, M., et al. (2015). Optimal inference with suboptimal models: Addiction and active Bayesian inference. *Medical Hypotheses*, 84, 109–117.
- Shafir, E., & Tversky, A. (1992). Thinking through uncertainty: Nonconsequential reasoning and choice. *Cognitive Psychology*, 24, 449–474.
- Simen, P., Cohen, J., & Holmes, P. (2006). Rapid decision threshold modulation by reward rate in a neural network. *Neural Networks*, 19, 1013–1026.
- Skinner, D., & Binney, J. (2014). *The physics of quantum mechanics*. Oxford University Press.
- Tversky, A. (1977). Features of similarity. *Psychological Review*, 84, 327–352.
- Tversky, A., & Kahneman, D. (1974). Judgment under uncertainty: Heuristics and biases. *Science*, 185, 1124–1131.
- Tversky, A., & Kahneman, D. (1983). Extension versus intuitive reasoning: The conjunction fallacy in probability judgment. *Psychological Review*, 90, 293–315.
- Tversky, A., & Shafir, E. (1992). The disjunction effect in choice under uncertainty. *Journal of Psychological Science*, 3, 305–309.
- Vedral, V. (2011). Living in a quantum world. *Scientific American*.
- Wichert, A., & Moreira, C. (2018). Balanced quantum-like model for decision making. In *Proceedings of the 11th international conference on quantum interactions*.
- Zadeh, L. (2006). Generalized theory of uncertainty (gtu) - principal concepts and ideas. *Computational Statistics & Data Analysis*, 51, 15–46.